MARTIN MARIETTA ENERGY SYSTEMS LIBRARIES

3 4456 0354277 1

ORNL/TM-11629

ornl

OAK RIDGE NATIONAL LABORATORY

MARTIN MARIETTA

Steady-State and Transient Tests Using the Unguarded Thin-Heater Apparatus (Thermophysical Properties of Building Materials)

D. L. McElroy
R. S. Graves
D. W. Yarbrough
H. A. Fine

OAK RIDGE NATIONAL LABORATORY
CENTRAL RESEARCH LIBRARY
CIRCULATION SECTION
4500N ROOM 175
LIBRARY LOAN COPY
DO NOT TRANSFER TO ANOTHER PERSON
If you wish someone else to see this report, send in name with report and the library will arrange a loan.

MANAGED BY
MARTIN MARIETTA ENERGY SYSTEMS, INC.
FOR THE UNITED STATES
DEPARTMENT OF ENERGY

This report has been reproduced directly from the best available copy.

Available to DOE and DOE contractors from the Office of Scientific and Technical Information, P.O. Box 62, Oak Ridge, TN 37831; prices available from (615) 576-8401, FTS 626-8401.

Available to the public from the National Technical Information Service, U.S. Department of Commerce, 5285 Port Royal Rd., Springfield, VA 22161.

This report was prepared as an account of work sponsored by an agency of the United States Government. Neither the United States Government nor any agency thereof, nor any of their employees, makes any warranty, express or implied, or assumes any legal liability or responsibility for the accuracy, completeness, or usefulness of any information, apparatus, product, or process disclosed, or represents that its use would not infringe privately owned rights. Reference herein to any specific commercial product, process, or service by trade name, trademark, manufacturer, or otherwise, does not necessarily constitute or imply its endorsement, recommendation, or favoring by the United States Government or any agency thereof. The views and opinions of authors expressed herein do not necessarily state or reflect those of the United States Government or any agency thereof.

ORNL/TM-11629

Metals and Ceramics Division

STEADY-STATE AND TRANSIENT TESTS USING THE UNGUARDED THIN-HEATER APPARATUS (THERMOPHYSICAL PROPERTIES OF BUILDING MATERIALS)

D. L. McElroy, R. S. Graves, D. W. Yarbrough, and H. A. Fine

Date Published: March 1991

NOTICE: This document contains information of a preliminary nature. It is subject to revision or correction and therefore does not represent a final report.

Prepared for
U.S. Department of Energy
Office of Building Energy Research
EC 01 01 00 0

Prepared by the
OAK RIDGE NATIONAL LABORATORY
Oak Ridge, TN 37831-6285
managed by
MARTIN MARIETTA ENERGY SYSTEMS, INC.
for the
U.S. DEPARTMENT OF ENERGY
Under Contract DE-AC05-84OR21400

MARTIN MARIETTA ENERGY SYSTEMS LIBRARIES

3 4456 0354277 1

TABLE OF CONTENTS

LIST OF TABLES v

LIST OF FIGURES vii

ABSTRACT 1

1. INTRODUCTION 2

2. OBJECTIVES 2

3. EQUIPMENT 4

3.1 STEADY-STATE MEASUREMENTS 4

3.2 TRANSIENT MEASUREMENTS 7

4. ANALYSIS OF TRANSIENT TESTS 10

4.1 METHOD 1:DATA TO 1800 s 10

4.2 METHOD 2:HEAT FLUX CHANGE 14

4.3 METHOD 3:THERMAL MASS CHANGE 14

5. TEST SPECIMENS 22

5.1 GYPSUM BOARDS 22

5.2 CALCIUM SILICATE BOARDS 25

5.3 WOOD PRODUCTS 27

5.4 PLASTIC CELLULAR FOAMS 29

6. TEST RESULTS 30

6.1 STEADY-STATE THERMAL CONDUCTIVITY VALUES 30

6.1.1 Gypsum boards 30

6.1.2 Calcium silicate boards 33

6.1.3 Wood products 35

6.1.4 Plastic cellular foams 36

6.2 TRANSIENT DATA ANALYSIS RESULTS 41

6.2.1 Gypsum boards containing wax 41

6.2.2 Calcium silicate boards 48

6.2.3 Wood products 50

6.2.4 Plastic cellular foams 54

7. DISCUSSION OF RESULTS 57

7.1 MEASURING EQUIPMENT AND ANALYSIS DEVELOPMENT 58

7.2 THERMOPHYSICAL PROPERTIES OF BUILDING MATERIALS 60

8. CONCLUSIONS AND RECOMMENDATIONS 64

8.1 CONCLUSIONS 64

8.2 RECOMMENDATIONS 66

9. ACKNOWLEDGMENTS 67

10. REFERENCES 68

APPENDIX A: FINITE DIFFERENCE MODEL EMPLOYED IN THE DEVELOPMENT OF METHOD 3 72

APPENDIX B: PROGRAM THAT PERFORMS THE ITERATIVE CALCULATIONS FOR MEHTOD 3 81

LIST OF FIGURES

Fig. 1. Schematic drawing of (*a*) the instrumented Nichrome screen wire heater and (*b*) the temperature control and plumbing systems for each cold plate 5

Fig. 2. Assembled unguarded thin-heater apparatus without perimeter insulation 6

Fig. 3. Temperature of the thin heater as a function of the square root of time (T1R). 11

Fig. 4. Comparison of complete transient solution (T_c) and short-time transient solution (T_{st}) 13

Fig. 5. Temperature response of the thin heater as a function of Fourier number and thermal mass ratio 15

Fig. 6. Values of the slope of the temperature rise of the heater as a function of thermal mass ratio 18

Fig. 7. Comparison of calculated and measured heater temperature changes for (a) gypsum (GOW), (b) calcium silicate (CS1), and (c) polystyrene 21

Fig. 8. Thermal conductivity at 24°C of calcium silicate as a function of specimen density (see Table 9) 27

Fig. 9. Thermal conductivity as a function of temperature for gypsum-wax specimens 32

Fig. 10. Thermal conductivity of three calcium silicate specimens as a function of temperature 34

Fig. 11. Thermal conductivity of three wood-product test specimens as a function of temperature 36

Fig. 12. Thermal conductivity as a function of temperature and time after manufacture for extruded polystyrene (HCFC-142b) and polyisocyanurate (CFC-11) 38

Fig. 13. Thermal conductivity at 24°C of extruded polystyrene (HCFC-142b) as a function of time after manufacture 39

Fig. 14. Natural logarithm of 100 *k* vs $(\text{time})^{1/2}$/thickness for the Massachusetts Institute of Technology model of aging by a plastic foam and Oak Ridge National Laboratory data on extruded polystyrene 40

Fig. 15. Specific heat as a function of temperature for gypsum-wax specimen 45

Fig. 16. Temperature vs time for gypsum without wax (GOW) and gypsum with 30 wt % wax (G30W) 46

Fig. 17. Specific heat as a function of temperature for three calcium silicate insulations 50

Fig. 18. Specific heat as a function of temperature for three wood products 52

Fig. 19. Specific heat as a function of temperature for cellular plastic foams 56

Fig. 20. Thermal conductivity as a function of temperature for four sets of materials 61

Fig. 21. Specific heat as a function of temperature for four sets of building materials 62

Fig. 22. Thermal diffusivity of four sets of building materials as a function of temperature form 20 to 50°C 63

LIST OF TABLES

Table 1. A comparison of Oak Ridge National Laboratory and National Bureau of Standards (1983) 7

Table 2. A comparison of Oak Ridge National Laboratory and National Institute of Standards and Technology (1990) 8

Table 3. Transient signals recorded by the Hewlett Packard system 8

Table 4. Recorded data for the first 30 min of a transient test (every fifth data point only) (T1R 032089) on gypsum board[a] 9

Table 5. Slopes for the least-squares fit lines to the linear region of temperature vs $(\text{time})^{0.5}$ curves 17

Table 6. Comparison of results for the different methods to calculate specific heat 20

Table 7. Building material test specimens for steady-state and transient tests in the Unguarded Thin-Heater Apparatus 23

Table 8. Estimated properties at 24°C for gypsum-wax test specimens 24

Table 9. Thermal conductivity values at 24°C as a function of density for calcium silicate insulation 26

Table 10. Estimated properties at 24°C for calcium silicate boards 27

Table 11. Average moisture contents of wood-product test specimen (wt %) 28

Table 12. Estimated properties at 24°C for wood-product test specimen 29

Table 13. Estimated properties at 24°C for plastic cellular foam test specimens 30

Table 14. Summary of *k*-values for GOW, G15W, and G30W test specimens 31

Table 15. Thermal conductivity values for three calcium silicate specimens as measured in the Oak Ridge National Laboratory unguarded thin-heater apparatus 33

Table 16. Thermal conductivity values for three wood products 35

Table 17. Thermal conductivity values as a function of temperature and time after production for extruded polystyrene foamed with HCFC 142b and polyisocyanurate foamed with CFC-11 37

Table 18. Specific heat values obtained by Methods 1 (1.1, 1.2) or 2, and 3 42

Table 19. Summary of specific heat (*C*) values from analysis of transient tests of gypsum-wax composites using Method 1.1 44

Table 20. Calculated thermal diffusivity for three gypsum-wax composites 47

Table 21. Summary of the thermophysical properties of calcium silicate derived from analysis of transient tests by Method 2 49

Table 22. Calculated thermal diffusivity for three calcium silicate specimens (α x 10^7, m^2/s) 50

Table 23. Summary of the thermophysical properties of wood products derived from analysis fo transient tests by Method 2. 51

Table 24. Calculated thermal diffusivity for three wood product specimens (α x 10^7, m^2/s) 53

Table 25. Summary of the thermophysical properties of cellular plastic foams from analysis of transient tests by Method 2 55

Table 26. Calculated thermal diffusivity for cellular plastic foams (α x 10^7, m^2/s) 56

Table 27. Summary of differences between calculation methods 57

Table 28. Specimen thermal mass and the thermal mass ratio (300 $J/m^3 \cdot K$) 58

Table 29. Thermal response parameters at 24°C for the building material test specimens 65

STEADY-STATE AND TRANSIENT TESTS USING THE UNGUARDED THIN-HEATER APPARATUS (THERMOPHYSICAL PROPERTIES OF BUILDING MATERIALS)*

D. L. McElroy, R. S. Graves, D. W. Yarbrough, and H. A. Fine†

ABSTRACT

The Oak Ridge National Laboratory unguarded thin-heater apparatus (UTHA) was used to determine the thermophysical properties [i.e., thermal conductivity (k), specific heat (C), and thermal diffusivity (α)] of building materials from 24 to 50°C (75 to 120°F). Steady-state and transient modes of operation yielded data on four types of material: (1) gypsum wallboard containing 0, 15, and 30 wt % wax; (2) calcium silicate insulations with densities (ρ) of 307, 444, and 605 kg/m^3; (3) three wood products [i.e., southern yellow pine flooring (575 kg/m^3), Douglas fir plywood (501 kg/m^3), and white spruce flooring (452 kg/m^3)]; and (4) two cellular plastic foams [i.e., extruded polystyrene (30 kg/m^3) blown with HCFC-142b and polyisocyanurate rigid board (30.2 kg/m^3) blown with CFC-11]. The extruded polystyrene was measured 25, 45, 74, 131, and 227 d after production.

In the steady-state mode of operation, the UTHA yields the k of the test specimen. In 1983 the uncertainty in k results by this absolute method was found to be less than ±2% by modeling, by a determinate error analysis, and by use of standard reference materials SRM 1450b and SRM 1451. These SRMs were retested in the UTHA in 1990, and agreement with the National Institute of Standards and Technology values was 0.3% for SRM 1451 and 1.1% for SRM 1450b. The UTHA k-values for the SRMs were fitted to better than 0.3% by a linear function of temperature. The UTHA k-values reported in this report provide an accurate description of the temperature dependency of k of several materials.

In the UTHA transient mode of operation, a step-change in heat flux was applied to specimens that were initially isothermal or that had a steady, imposed temperature gradient. Hewlett Packard 9121 computer was used to control the test and to record the temperature-time behavior of the thin heater. Analysis of the temperature response of the thin heater for short times predicts a temperature rise that is a linear function of the square root of time. This behavior was observed, and the slope of this relation provided experimental values for the product $k \bullet \rho \bullet C$. The overall error in determining the the product

---

*Research sponsored by the U.S. Department of Energy, Assistant Secretary for Conservation and Renewable Energy, Office of Buildings Energy Research, Building Systems and Materials Division, under contract DE-AC05-84OR21400 with Martin Marietta Energy Systems, Inc.

†Department of Materials Science and Engineering, University of Kentucky, Lexington.

$k \bullet \rho \bullet C$ is less than 1%. Values of C were calculated from experimental values of k, ρ, and the product of $k \bullet \rho \bullet C$. For the materials with densities above 300 kg/m^3, the thermal response and transient analysis described above was applicable. However, for the 30 kg/m^3 foams, the thermal mass of the thin heater delayed the onset of the linear temperature rise with the square root of time. This effect negated the use of the short-time transient analysis for low-density materials. A finite difference program that described this observation provided an alternate method to obtain values for the product $k \bullet \rho \bullet C$ from the experimental data. Valuable design information for future UTHA equipment was also obtained from this alternate analysis. For each of the tested materials, the experimental values of k, ρ, and C and their dependency on temperature are compared with literature values. In addition, these experimental values were used to calculate thermal diffusivity ($\alpha = k/\rho \bullet C$) and its dependency on temperature.

---

1. INTRODUCTION

This report describes use of the Oak Ridge National Laboratory (ORNL) unguarded thin-heater apparatus (UTHA) in the steady-state and transient modes of operation to determine thermophysical properties [i.e., thermal conductivity (k), specific heat (C), and thermal diffusivity (α)] of building materials from 24 to 50°C (75 to 120°F). These properties were determined for (1) gypsum wallboard containing 0, 15, and 30 wt % wax; (2) calcium silicate insulations with densities (ρ) of 307, 444, and 605 kg/m^3; (3) three wood products [i.e., southern yellow pine flooring (575 kg/m^3), Douglas fir plywood (501 kg/m^3), and white spruce flooring (452 kg/m^3); and (4) two cellular plastic foams [i.e., extruded polystyrene (30 kg/m^3) blown with HCFC-142b and polyisocyanurate rigid board (30.2 kg/m^3) blown with CFC-11]. The extruded polystyrene was measured 25, 45, 74, 131, and 225 d after production. Discussed are the objectives of this study, the UTHA, the steady-state and transient modes of operating the UTHA, the analyses of results obtained with the UTHA, the characteristics of the test specimens, the test results obtained, a comparison of the test results with previous studies, conclusions, and recommendations for future research.

2. OBJECTIVES

The need for transient analysis of buildings has increased interest in measuring the nonsteady-state thermal behavior of building materials. Transient analysis is possible with the

ORNL UTHA because the heat capacity of the screen heater is small relative to that of commonly used measurement systems. One purpose of this study was to demonstrate the transient mode of operation of the UTHA to obtain thermophysical properties of building materials. The UTHA is described in Sect. 3.

The primary use of the UTHA has been in the steady-state mode of operation as a means to determine the apparent thermal conductivity (k) of building insulations from 24 to 50°C. The intent of this study was to obtain data during the nonsteady-state condition that precedes the steady-state condition and to interpret these data to obtain other physical properties of the test specimen. Doing so provided the opportunity to reexamine test and analysis results that were produced during the development of the UTHA.

The use of the UTHA in the steady-state and transient modes of operation was also prompted by the need to test gypsum board specimens containing 0, 15, or 30 wt % wax (i.e., $C_{18}H_{38}$, n-octadecane) in the temperature range of 20 to 50°C. These tests were part of an effort to develop a gypsum wall board with enhanced thermal storage capacity. The wax, which melts and freezes near room temperature, provides a phase-change material that can be added by suffusion into the open pore spaces of the gypsum board. The objective of the thermal tests was to develop thermophysical property data for gypsum board and gypsum-wax composites and to study their transient thermal performance using the UTHA.

The transient tests on the gypsum boards containing wax showed the potential value of applying this technique to other building materials to develop a thermophysical-property data base. This opportunity was explored as specimens became available that allowed two-sided heat-flow tests. Tests were conducted on three calcium silicate insulations, three wood products, and two cellular plastic foams as a function of time after production. This report compares results on these materials with previously published values.

The transient tests on the low-density (30 kg/m^3) extruded polystyrene and a polyisocyanurate foamed with CFC-11 yielded a temperature response of the thin heater different from that for materials with densities above 300 kg/m^3. This finding prompted a reexamination of the analysis of the transient data and yielded valuable design information for future UTHA equipment.

3. EQUIPMENT

3.1 STEADY-STATE MEASUREMENTS

The UTHA is an absolute longitudinal heat flow technique having less than 2% uncertainty for steady-state thermal resistance tests between 20 and 80°C. In this technique a constant heat flux is provided by a dc-powered, instrumented, Nichrome,* screen wire heater located between two temperature-controlled copper plates. Large area (0.9- by 1.5-m) flat specimens are located between the heater and each plate. For two-sided heat flow k is calculated from

$$k = \frac{I \cdot \Delta V}{2} \cdot \frac{L}{A \cdot \Delta T} , \tag{1}$$

where I = current through the screen (amps),

ΔV = voltage drop along the screen (volts),

L = average specimen thickness (m),

A = screen area defined by its width and the voltage lead separation (m^2),

ΔT = temperature difference (in Kelvin) between the screen and the plates.

Detailed descriptions of the technique have been published.[1-6] The American Society for Testing and Materials (ASTM) approved this technique as a standard test method on April 8, 1989 (ref. 6). Figure 1 is a schematic drawing of the instrumented Nichrome screen wire heater and the temperature control and plumbing for the cold plates. Figure 2 shows the assembled UTHA without perimeter insulation.

A determinate error analysis for the quantities given in Eq. (1) has shown that the total uncertainty is ±1.7% for an assumed temperature difference of 10°C.[4] The most probable uncertainty is near ±1.2%. The reproducibility and repeatability of the k measurements have been determined to be ±0.2%.[5]

In 1983, tests were conducted on two standards from the National Bureau of Standards (NBS) [now the National Institute of Standards and Technology (NIST)]; Table 1 shows these results.[5] The ORNL results on the NBS Certified Transfer Standard were within 0.6% of NBS values at 303 and 313 K (30 and 40°C). ORNL measurements from 22 to 60°C on

---

*Nichrome is a trade name of Driver-Harris Company for an 80 nickel-20 chromium alloy.

ORNL-DWG 82-16959

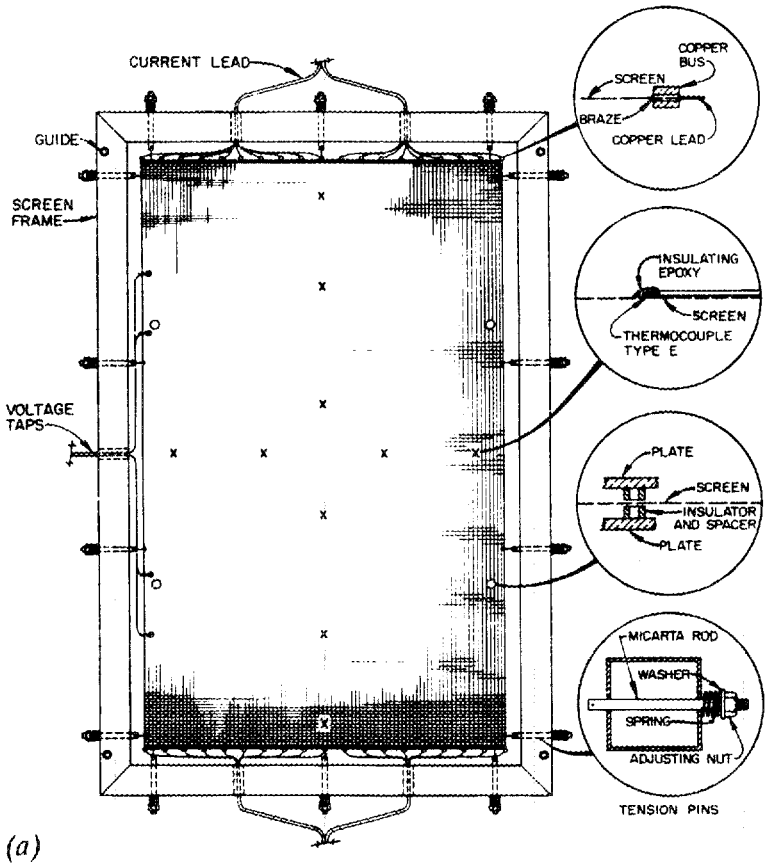

(a)

ORNL- DWG 83-14363

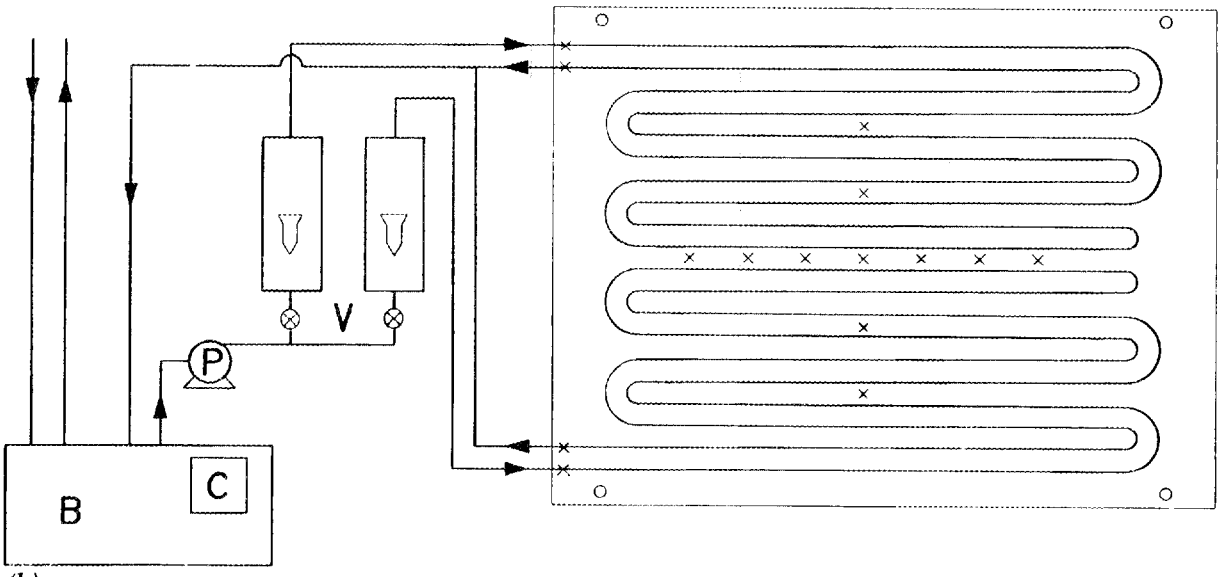

(b)

Fig. 1. Schematic drawing of (*a*) the instrumented Nichrome screen wire heater and (*b*) the temperature control and plumbing systems for each cold plate.

Y186572

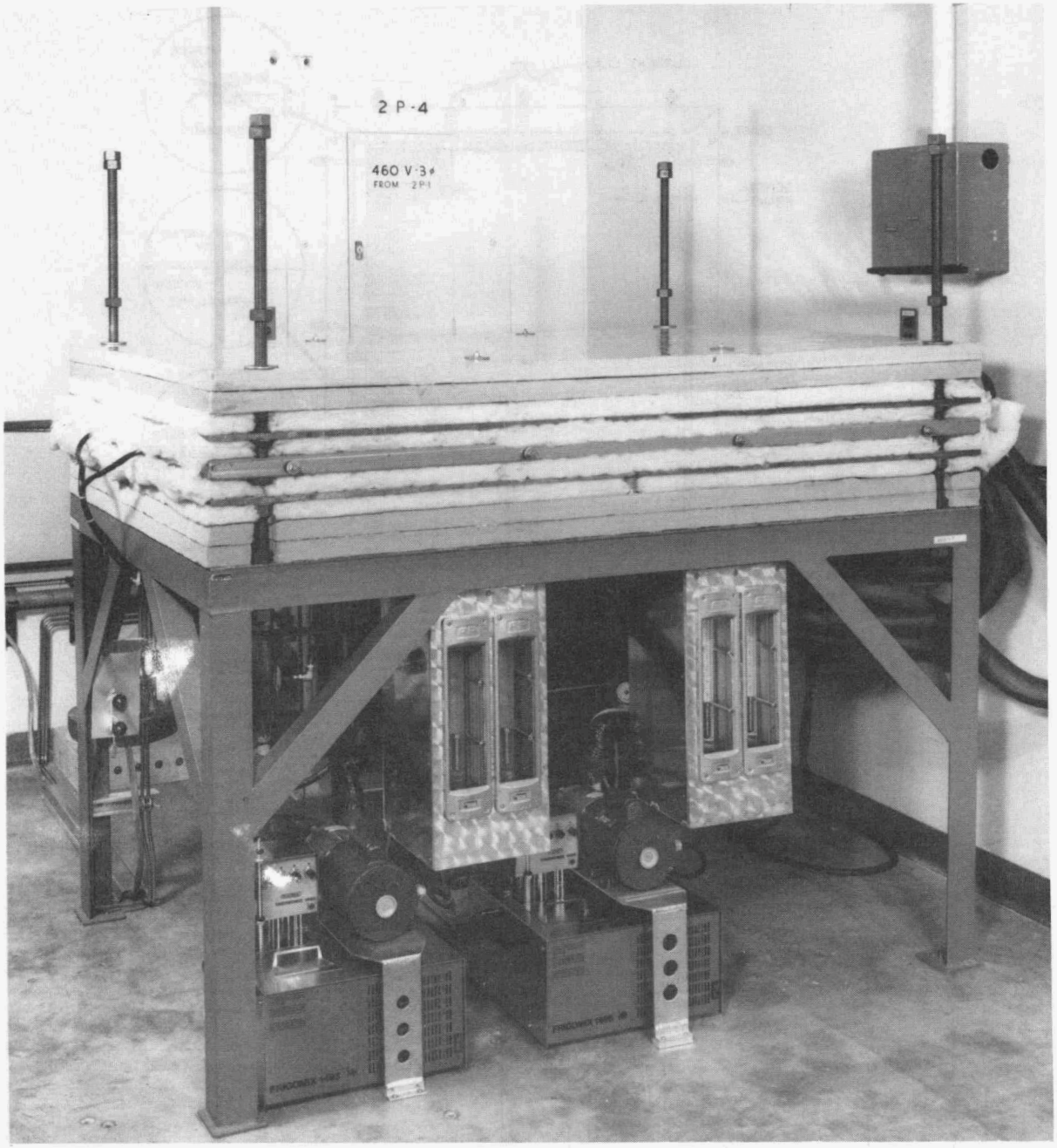

Fig. 2. Assembled unguarded thin-heater apparatus without perimeter insulation.

Table 1. A comparison of Oak Ridge National Laboratory and National Bureau of Standards (1983)

Specimen	Mean sample temperature (K)	Sample density (kg/m^3)	*k*-ORNL (W/m•K)	*k*-NIST (W/m•K)	Difference[a] (%)
Certified transfer standard					
Two-sided	303.14	9.255	0.04813	0.04827	-0.29
	313.14	9.270	0.05164	0.05166	-0.04
One-sided	303.23	9.350	0.04811	0.04809	0.04
	303.23	9.340	0.04808	0.04835	-0.56
SRM 1450b					
Two-sided (14 points)	297.13	127.0	0.03454	0.03485	-0.89
(13 points)			0.03466	0.03485	-0.55

[a]100•[(*k*-ORNL) - (*k*-NBS)]/(*k*-NBS).

standard reference material SRM 1450b yielded a maximum difference of 0.9% between measurements by the two laboratories at 297.13 K. These SRMs were retested in theUTHA in 1990 (Table 2); agreement with the NIST values was 0.3% for SRM 1451 and 1.1% for SRM 1450b. The UTHA *k*-values for the SRMs were fitted to better than 0.3% by a linear function of temperature. Because all of these comparisons are within the most probable uncertainty of 1.2%, the UTHA *k*-values reported here provide an accurate description of the temperature dependency of *k* of several materials.

3.2 TRANSIENT MEASUREMENTS

Transient tests can be performed in the UTHA as a two-sided test by applying a step-change in heat flux to an initially isothermal specimen or to a specimen with a steady-state temperature gradient. The temperature of the heater increases with time at a rate that depends on the applied power, the thermal properties of the test specimen and the heater, and the temperature of the cold plates. The resulting temperature-time behavior of heater can be analyzed to obtain specimen properties.[3,7]

Table 2. A comparison of Oak Ridge National Laboratory and National Institute of Standards and Technology (1990)

Specimen	Mean sample temperature (K)	Sample density (kg/m^3)	k_a-ORNL (W/m•K)	k_a-NIST (W/m•K)	Difference[a] (%)
Certified transfer standard, SRM 1451					
Two-sided	303.14	9.255	0.04829	0.04827	0.04
	313.14	9.270	0.05180	0.05166	0.27
SRM 1450b					
Two-sided (4 points)	297.13	127.0	0.03445	0.03485	-1.14

[a]$100[(k_a\text{-ORNL}) - (k_a\text{-NIST})]/(k_a\text{-NIST})$.

A Hewlett Packard (HP) 9121 computer was used to control the test and to record data.[8] Table 3 lists the types of data logged by an HP 3497A data acquisition system. The average heater temperatures were determined from the readings of five thermocouples located at the center of the heater. The electromotive force of each thermocouple was measured to 1 μV

Table 3. Transient signals recorded by the Hewlett Packard system

Number	Type signal	Symbol
11	Thermocouples on the screen heater	TSA[a]
5	Thermocouples on the upper plate	TTPC
5	Thermocouples on the lower plate	TBPC
1-10	Thermocouples located within the specimen	TSCU1
2	Voltage drops,[b] 0.6 and 0.9 m	VS24
1	Current reading[b]	CS

[a]TSA: Average temperature for five thermocouples on the screen.

[b]PS: Calculated from VS (0.6 m) by CS/0.557 m^2. Heat flux W/m^2.

and converted to temperature using a calibration table.[9] After the procedure was developed, data were recorded every 12 s from 10 min prior to changing the power until 60 min after the power was changed, then every 120 s for the next 300 min, and then every 300 s until steady-state condition was achieved. The software allows 1000 points to be recorded. Table 4 is a printout of the first 30 min of a transient test on the gypsum board. For each specimen the first transient test was conducted on an isothermal specimen with the initial temperature difference between the plates and the screen less than 0.05°C for plate temperatures between 25 and 50°C. At the conclusion of the first transient test, a steady-state measurement was made of the specimen *k*. The second transient test was initiated with a temperature gradient on the specimen and was followed by another steady-state measurement of the specimen *k*. This procedure was repeated to obtain three or four heating transient tests on most specimens. Finally, a cooling transient test was conducted by a step-change in the heat flux to zero.

Table 4. Recorded data for the first 30 min of a transient test (every fifth data point only) (T1R 032089) on gypsum board[a]

TIME	TSA	TTPC	TBPC	TSCU1	TSCD1	PS
829	20.97	20.98	20.95	21.05	21.00	0
877	20.95	20.97	20.95	21.03	20.98	0
937	21.46	20.97	20.95	21.05	21.00	41.280
997	21.71	20.97	20.95	21.05	21.00	41.283
1057	21.87	20.97	20.97	21.05	21.00	41.282
1117	22.00	20.97	20.95	21.05	21.02	41.279
1177	22.11	20.97	20.93	21.07	21.03	41.279
1237	22.23	20.98	20.95	21.07	21.03	41.275
1297	22.32	20.97	20.95	21.08	21.07	41.277
1357	22.42	20.98	20.97	21.12	21.10	41.278
1417	22.51	20.98	20.97	21.12	21.10	41.275
1477	22.57	20.97	20.95	21.13	21.15	41.275
1537	22.65	20.98	20.95	21.15	21.18	41.275
1597	22.72	20.98	20.97	21.20	21.22	41.275
1657	22.79	20.97	20.95	21.22	21.25	41.275
1717	22.86	20.97	20.95	21.23	21.28	41.277
1777	22.94	20.98	20.97	21.25	21.32	41.277
1837	22.99	20.97	20.95	21.28	21.33	41.278
1897	23.04	20.97	20.95	21.32	21.38	41.278
1957	23.11	20.98	20.95	21.33	21.42	41.278
2017	23.16	20.98	20.97	21.38	21.45	41.279
2077	23.23	20.98	20.97	21.38	21.48	41.280
2137	23.27	21.00	20.97	21.43	21.53	41.276
2197	23.32	20.97	20.95	21.43	21.55	41.277
2257	23.36	20.97	20.95	21.47	21.58	41.278
2317	23.42	20.98	20.97	21.50	21.62	41.279
2377	23.47	20.97	20.95	21.53	21.65	41.279
2437	23.53	20.98	20.97	21.55	21.68	41.280
2497	23.56	20.98	20.95	21.58	21.72	41.280
2557	23.62	20.98	20.95	21.62	21.75	41.280
2617	23.65	20.97	20.95	21.63	21.78	41.280
2677	23.71	20.98	20.97	21.68	21.81	41.280
2737	23.74	20.97	20.95	21.68	21.83	41.274
2773	23.78	20.98	20.97	21.70	21.86	41.274

[a]See Table 3 for explanation of terms; time in seconds, T in °C, PS in W/m^2.

4. ANALYSIS OF TRANSIENT TESTS

4.1 METHOD 1: DATA TO 1800 s

A solution of the conduction equation of heat transfer is given by Carslaw and Jaeger[10] for the case of a semi-infinite solid that is initially at constant temperature, T°, and that is subjected to a constant heat flux, F, at the surface $x = 0$ for time $(t) \geq t_0$. The temperature-time relationship at any surface x within the material is given by

$$T = T^o + \frac{2F}{k}[\alpha(t - t_0)]^{1/2}\ ierfc\left(\frac{x}{2[\alpha(t - t_0)]^{1/2}}\right) . \tag{2}$$

At $x = 0$ (the heater),

$$T = T^o + \frac{2F}{k}\left[\frac{\alpha}{\pi} \cdot (t - t_0)\right]^{1/2} . \tag{3}$$

For a short time interval the above equations for a semi-infinite material are applicable to a material of finite thickness (L), such as the samples in the UTHA transient experiment. During this short time interval the temperature near the surface x equal L remains nearly unaffected by the constant heat flux (F) at x equal zero. The short time interval for the denser materials of interest in the current work is about 1800 s. In the current work the temperature vs time and the heat flux are measured, so Eq. (4) allows the quantity $k\rho C$ to be determined from the slope of a least squares fit of the temperature vs $(t - t_0)^{1/2}$ data.

Equation (3) can be arranged as follows:

$$T = T^o + \frac{2F}{(\pi k\rho C)^{1/2}}\ (t - t_0)^{1/2} . \tag{4}$$

Thus a linear least-squares fit of the heater temperature as a function of $(t - t_0)^{1/2}$ is the same as Eq. (4) if

$$T = A + B\ (t - t_0)^{1/2} , \tag{5}$$

where A is a constant equal to the initial heater temperature T°, and B is the slope and equals $2F/(\pi k\rho C)^{1/2}$.

Equations 2 and 3 are for a material that is initially at uniform temperature. The principle of superposition, however, allows the solution to be extended to a material that has an initial temperature gradient. In the determination of $k\rho C$ using Eq. (4) with a temperature gradient, F equals the change in heat flux applied at time t_0. For a two-sided test, the change in heat flux is $F/2$.

Figure 3 shows that the experimentally determined heater temperature rise is a linear function of (time)$^{1/2}$ after the heat flux was changed for a transient test (T1R) on a gypsum

ORNL-DWG 17128

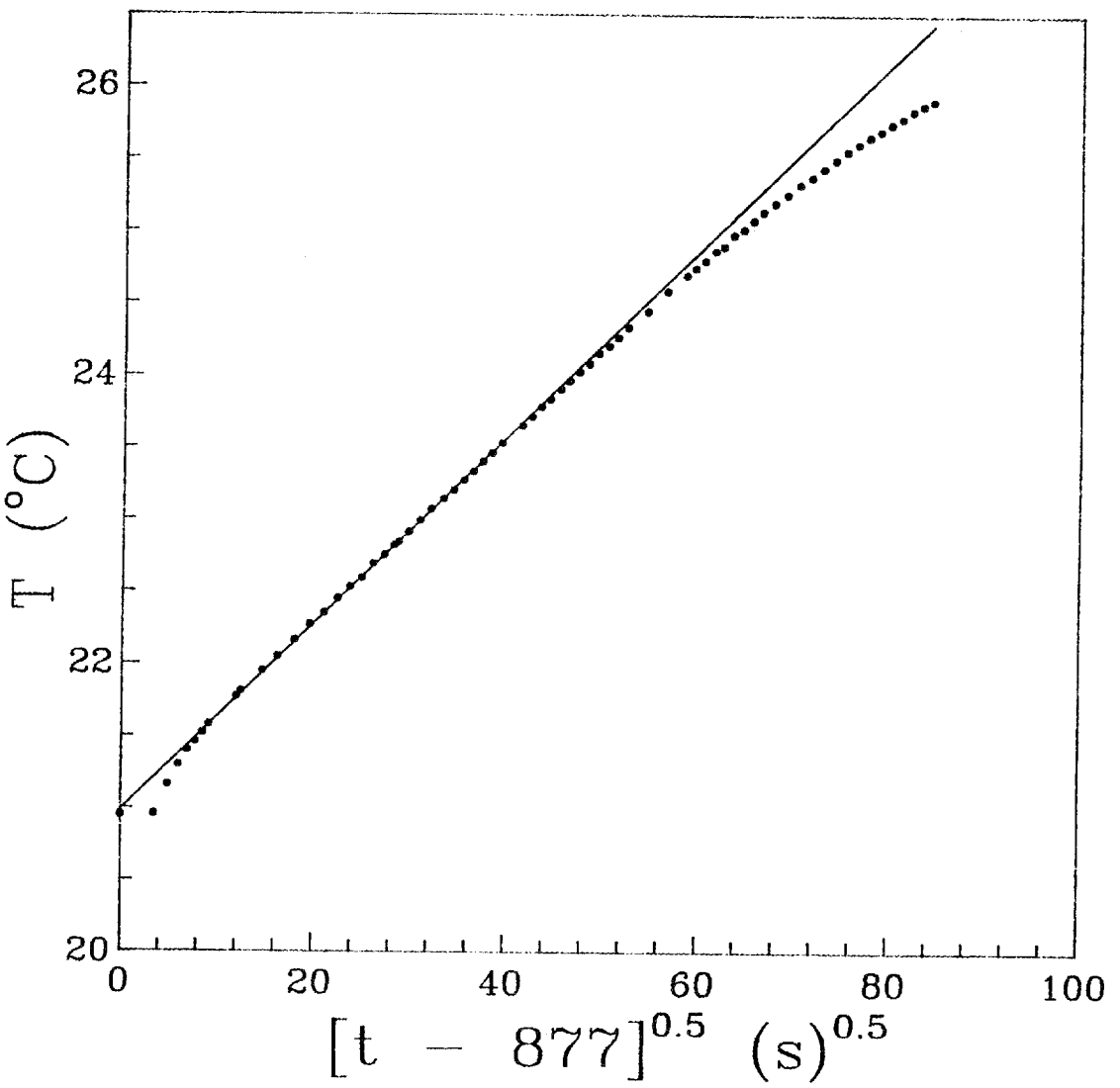

Fig. 3. Temperature of the thin heater as a function of the square root of time (T1R).

board. Table 4 contains these data. A least-squares fit of 151 points between 877 and 2689 s yielded

$$T = 20.96 + 0.06446\ (t - 877)^{1/2} \tag{6}$$

with an average percent deviation of less than 0.06%. The T° value of 20.96°C is within 0.01°C of the average cold plate temperature of 20.97°C. The slope term and the heat flux change of 41.281 W/m^2 yield a $k\rho C$ value of 13,0560 W^2•m^2/K^2; this yields a C value of 1055 J/kg•K for this specimen with a k of 0.178 W/m•K and ρ of 695.1 kg/m^3. Sections 6 and 7 of this report present results on other materials and a discussion of these results.

Two procedures were used for analysis of transient data. Method 1.1 for the denser materials used the complete data set for times from 200 to 1800 s after the heat flux change, and as described above, this included up to 151 data points. Method 1.2 used only 10 data points selected in uniform time increments from the complete data set for the same period. Method 1.2 yielded coefficients within 1% of those of Method 1.1.

Several sources of indeterminate error arise in the analysis of the transient tests. The development of Eqs. (2) and (3) assumes that the heat flux is constant. During the transient, however, the thin heater of the experimental apparatus undergoes a significant temperature change. As this heater has a small but significant mass, some of the power generation is used to increase the sensible heat of the heater. This error was illustrated in the analysis of the results as a small offset of approximately 0.03°C between the known initial temperature and that resulting from the least-squares analysis (see Fig. 3). This effect has been discussed by Domingos and Voelker.[11]

The applicability of the short-time solution for a semi-infinite specimen, Eq. (3), for the analysis of data was verified by comparison of the complete solution to the heat transfer problem with that for the short-time solution. Figure 4 shows the results of this calculation; the temperature of the complete solution, T_c, is plotted vs that for the short-time solution, T_{st}. Deviation from the straight line of slope one begins to occur at 1800 s. At 1800 s the short-time solution prediction for temperature is less than 1 mK too low. This error rises to 20 mK at 3600 s. Least-squares linear regression analysis of the data show that at 1800 s the slope of the line through the origin is 0.9999. This slope continues to decrease as points corresponding to longer times are added in the analysis. At 3600 s the slope equals 0.9961. The calculated value of $k\rho C$ is dependent on the square of the slope, so the resulting error was 0.01% at

ORNL-DWG 17160

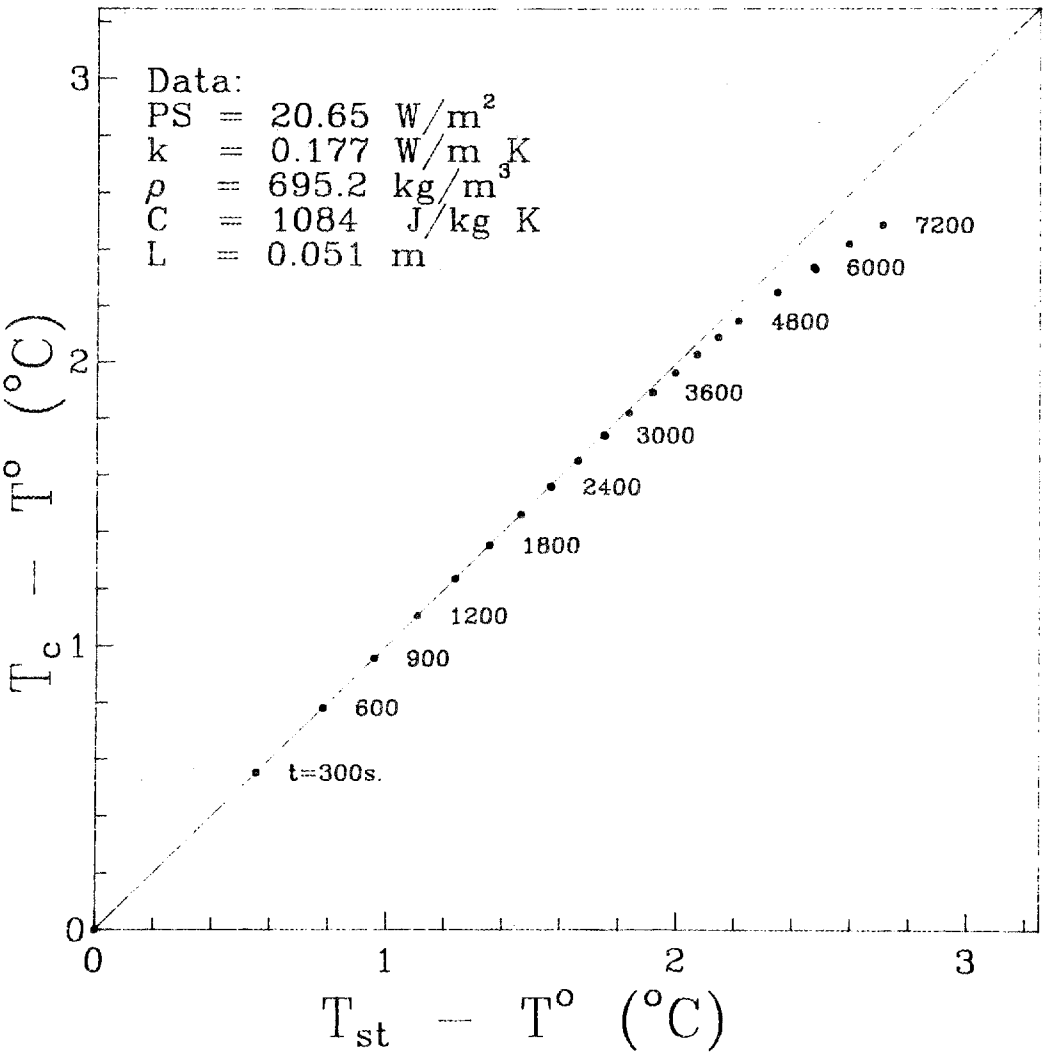

Fig. 4. Comparison of complete transient solution (T_c) and short-time transient solution (T_{st}).

1800 s and 0.8% at 3600 s. Allowing the least-squared line to have a nonzero intercept approximately doubled these errors. To minimize this error, the limit of applicability of the short-time solution for the materials of interest was, therefore, taken as 1800 s for the gypsum specimens (see Sect. 4.3 for other materials).

The most significant determinate error arose from the fact that the starting time for the initial experiments on the gypsum specimens with zero and 30% wax was only known to ±6 s. Analysis of the temperature-time results was thus performed for several values of t_0 and the

values of the slope set equal to that which yielded the "correct" initial starting temperature. Analysis of the results for the gypsum specimen with 15% wax for which the initial time was accurately known showed that an error of ±1 s would produce an error in the results of approximately ±0.4%; a ±3 s error yielded an error of ±0.7%, and a ±6 s error caused a ±1.1% error. The procedure employed allowed the initial time to be estimated to within ±1 s, so the error should be about ±0.4%. This analysis was confirmed by the agreement of the C values for gypsum.

The results of the transient experiments show very good agreement for the values of $k\rho C$ for each material. This suggests that all of the errors are small compared with that resulting from the initial time. Thus the overall error in $k\rho C$ is less than ±1% for gypsum specimens.

4.2 METHOD 2: HEAT FLUX CHANGE

This method of analyzing transient data was used after tests on low-density (30-kg/m^3) extruded polystyrene yielded a temperature response of the thin heater that was delayed in time. This time lag was associated with the thermal mass of the heater. To reduce the effect of this time lag, the step-change in heat flux was corrected:

$$F(corrected) = F - F_1 = F - \frac{dT}{dt}\left[\frac{x}{2} \cdot \rho \cdot C\right] \qquad (7)$$

$$= F - 303.79 \cdot \frac{dT}{dt},$$

where dT/dt is the rate of temperature change of the heater (K/S),

ρ is the heater density (2115 kg/m^3),

C is the heater specific heat (435 J/kg•K),

$x/2$ is half the heater thickness (330 x 10^{-6} m).

4.3 METHOD 3: THERMAL MASS CHANGE

This method of analyzing the transient data evolved from Method 2. It is based on a finite difference model of the transient behavior of an infinite slab of thickness L and a thin heater of thickness 0.5 t_{sc}. The boundary of the slab at x equal L is maintained at constant temperature $T(0)$. The boundary at x equal zero is in intimate contact with the thin heater. The heater has a finite thermal mass, 0.5 $t_{sc} \bullet \rho_{sc} \bullet C_{sc}$, and high thermal conductivity relative to

the slab. The slab may initially be isothermal or have a linear temperature gradient. The model yields the heater temperature vs time relationship for a given step-change in the power to the heater. The complete development of the model, which employs the implicit method, and the program are presented in Appendix A.

Dimensional analysis of this problem yields four dimensionless numbers:

1. dimensionless position, $X = x/L$;
2. Fourier number (or dimensionless time), $N_{Fo} = \alpha t/L^2$;
3. dimensionless temperature, $\hat{T} = [T(t) - T(0)]/[T(\infty) - T(0)]$; and
4. thermal mass ratio, TMR $= 0.5\ t_{sc} \bullet \rho_{sc} \bullet C_{sc}/L \bullet \rho \bullet C$.

Thus results for the heater temperature (i.e., the temperature at x equal 0) may be presented as a function of N_{Fo} and TMR. Figrue 5 presents some typical temperature response curves for the heater as a function of the square root of N_{Fo}.

The zero-heater-thermal-mass case (i.e., TMR equal zero) corresponds to Method 1. At short times a linear dependence of the heater temperature on the square root of time must, therefore, occur. Figure 5 shows this behavior for times corresponding to N_{Fo} less than approximately 0.5.

ORNL-DWG 17159

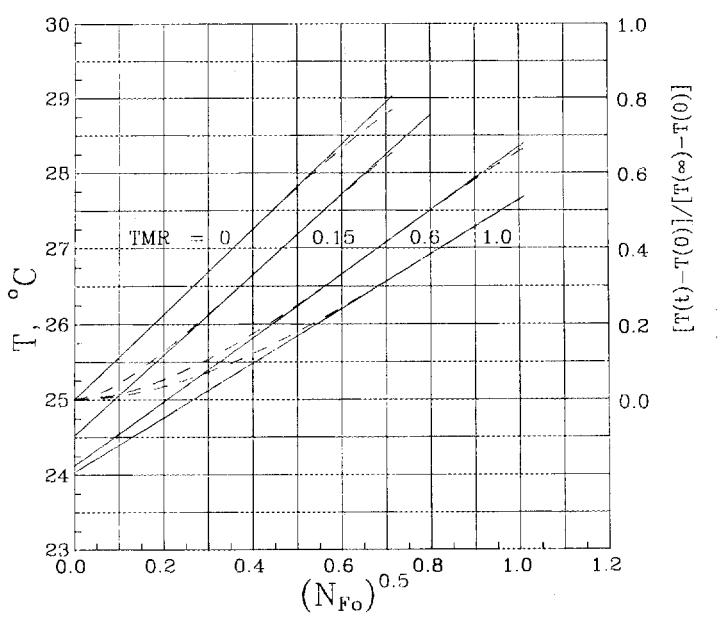

Fig. 5. Temperature response of the thin heater as a function of Fourier number and thermal mass ratio.

As the TMR increases, a nonlinear regime in the relationship between temperature and the square root of time occurs at short times. The length of this regime increases as TMR increases. In all cases the nonlinear regime is followed by a linear region. The linear region is then followed by a roll-off in temperature, as was the case for TMR equal zero. The onset of the linear region occurs at dimensionless times ranging from zero for TMR equal zero, to 0.36 ($N_{Fo}^{0.5} = 0.6$) for TMR equal 1. The end of the linear region occurs at N_{Fo} equal 0.25 for TMR equal zero and at N_{Fo} greater than 1 for TMR equal 1. For TMR less than or equal to 1, however, the linear region occurs for *dimensionless temperatures* between 0.3 and 0.5 (Fig. 5).

The slopes of the dimensionless heater temperatures vs the square root of dimensionless time curves are a function of the TMR and dimensionless time. In the linear region between dimensionless temperatures of 0.3 and 0.5, the slope is solely a function of TMR:

$$\frac{dT}{d(N_{Fo})^{0.5}} = \frac{d\,\{[T(t) - T(0)]/[T(\infty) - T(0)]\}}{d(\alpha t/L^2)^{0.5}} = f(TMR) \;@\; 0.3 \le T \le 0.5$$
$$= \frac{L}{[T(\infty) - T(0)]\;\alpha^{0.5}]} \;\frac{d\,T(t)}{d\,t^{0.5}}\,. \tag{8}$$

The ratio of the slope for any TMR to that for TMR equal zero then equals

$$\frac{\left[\dfrac{L}{[T(\infty) - T(0)]\;\alpha^{0.5}}\;\dfrac{dT(t)}{dt^{0.5}}\right]_{TMR} = \left[\dfrac{dT(t)}{dt^{0.5}}\right]_{TMR}}{\left[\dfrac{L}{[T(\infty) - T(0)]\;\alpha^{0.5}}\;\dfrac{dT(t)}{dt^{0.5}}\right]_{TMR_{=0}} = \left[\dfrac{dT(t)}{dt^{0.5}}\right]_{TMR_{=0}}} \tag{9}$$
$$= \frac{S(TMR)}{S(0)}\,,$$

where S(TMR) and S(0) designate the slopes of the heater temperature vs the square root of time curve in the range of dimensionless temperature between 0.3 and 0.5 for any TMR and for TMR equal zero respectively. Assuming the ratio S(TMR)/S(0) may be expressed as a polynomial in TMR yields

$$\frac{S(TMR)}{S(0)} = 1 + a\,TMR + b\,(TMR)^2 + \cdots\,. \tag{10}$$

The zero-heater-thermal-mass analysis, Method 1, yielded

$$S(0) = F/(\pi \rho k C)^{0.5} \ . \tag{11}$$

A combination of Eqs. (10) and (11) yields

$$C = \left[\frac{F/(\pi \rho k)^{0.5}}{S(TMR)} \left(1 + a\ TMR + b\ (TMR)^2 + \cdots\right) \right]^2 . \tag{12}$$

The constants in the polynomial used to describe the dependence of the slope on TMR were established from least-squares fit straight lines to the heater temperature vs the square root of time results for a series of calculations. Table 5 and Fig. 6 show the values of these slopes and the resulting polynomials.

Table 5. Slopes for the least-squares fit lines to the linear region of temperature vs $(\text{time})^{0.5}$ curves

TMR	S(TMR)	S(TMR)/S(0)
0.00	1.1281[a]	0.999752
0.01	1.12702	0.998795
0.025	1.12223	0.994550
0.05	1.11665	0.989605
0.1	1.09372	0.969284
0.15	1.06593	0.944655
0.2	1.0376	0.919549
0.25	1.00946	0.894610
0.3	0.98284	0.871019
0.35	0.95671	0.847862
0.4	0.93068	0.824793
0.45	0.90803	0.804720
0.5	0.88661	0.785737
0.55	0.86588	0.767366
0.6	0.84687	0.750518
0.65	0.82723	0.733113
0.7	0.81014	0.717967
0.75	0.79384	0.703522
0.8	0.77817	0.689635
0.85	0.76402	0.677095
0.9	0.74908	0.663854
0.95	0.73592	0.652192
1	0.72347	0.641158

[a]S(0) equals 1.128379 from Eq. (11).

ORNL-DWG 17161

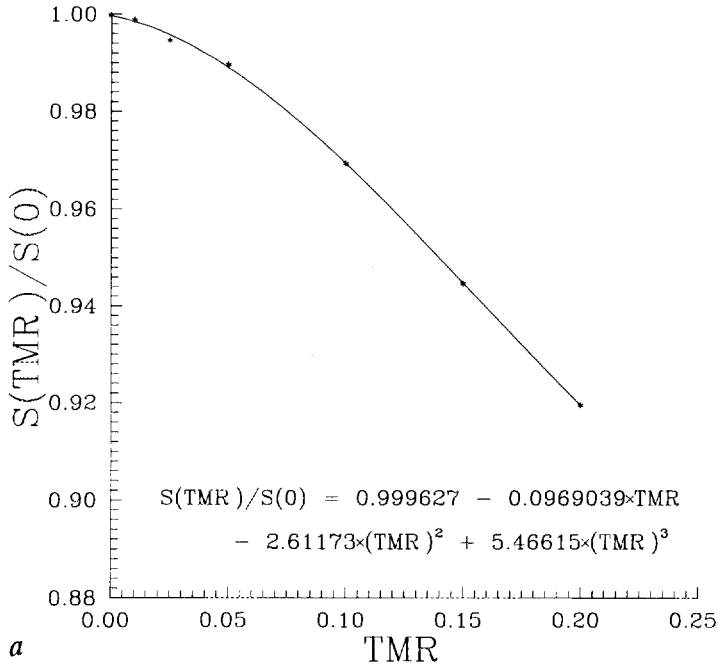

a

ORNL-DWG 17162

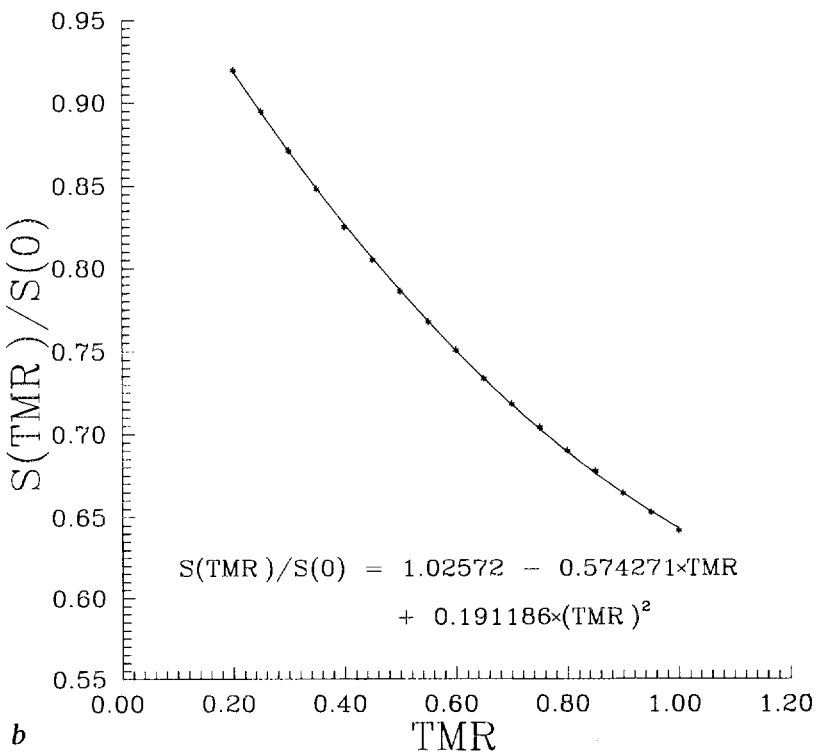

b

Fig. 6. Values of the slope of the temperature rise of the heater as a function of thermal mass ratio.

An iterative technique was then employed to solve Eq. (12), as C appears on both sides of the equation (i.e., on the left as C and on the right in the denominator of TMR). The iterative solution technique starts with a guess for C equal to $\{F/[(\pi \bullet \rho \bullet k)^{0.5}\ S(TMR)]\}^2$. This value for C is then used to calculate a value for TMR. The value for TMR is then used to find a new value for C using Eq. (12). The iteration continues until the new C and old C values agree to 0.001%. The program, which performs the iterative solution of Eq. (12), is given in Appendix B.

The curve for zero thermal mass ratio in Fig. 5 shows a linear dependence for the square root of dimensionless time less than approximately 0.5. The more detailed analysis performed for Method 1 presented in Sect. 4.2 shows an error of -0.01% at 1800 s and -0.8% at 3600 s. For the conditions stated in Fig. 4, these times correspond to dimensionless times of 0.1625 and 0.325 respectively. A linear fit to dimensionless time equal 0.25 would yield an error in the slope of -0.24% or an error in C of 0.5%.

Method 3 used the dimensionless temperature range between 0.3 and 0.5 to establish the slope, S(TMR). At zero thermal mass this criterion would correspond to dimensionless times between zero and approximately $(0.44)^2$ or 0.19. Based on the data used to construct Fig. 4, this slightly longer time interval would produce an error in the slope of -0.05% or 0.1% in C.

The difference between the specific heats from Method 3 and from Method 1 may, in part, be explained by the fact that Method 1 should be done at dimensionless times less than the specified value of 0.1625. The denser gypsum plus wax would, therefore, require longer times to be included in the analysis. The less dense materials, especially the plastic foams, would require much shorter times to be used. Table 6 shows the magnitude of the possible error. This error is further compounded by the small sample thickness used for the polyisocyanurate (PIR) with CFC-11. The approximately 40% reduction in thickness of this material would necessitate a 64% reduction in the time interval. The rollover at longer times results in a lower slope and thus higher C. This result could explain the large negative deviation (i.e., C from Method 2 greater than from Method 3). The larger slope at shorter times would make C lower for Method 2 for the PS samples and would make the error larger. A similar trend would result for all of the other materials except Douglas fir plywood.

Figure 5 suggests that the dimensionless temperature range that should be used in Method 3 is 0.3 to 0.5. This is based on the visual observation of the deviation from linearity. The slopes shown in Table 6 for other temperature ranges show, however, that the slope is

Table 6. Comparison of results for the different methods to calculate specific heat

Exp. No.	Method	Range	Slope	C (J/kg•K)
G32089		Gypsum		
	1	$t = 0 \rightarrow 1800$ s	0.06448	1054
		$t = 60 \rightarrow 1800$ s	0.06350	1087
		$t = 120 \rightarrow 1800$ s	0.06325	1096
	3	$\bar{T} = 0.3 \rightarrow 0.5$	0.06274	1111
		$\bar{T} = 0.3 \rightarrow 0.4$	0.06292	
		$\bar{T} = 0.4 \rightarrow 0.5$	0.06231	
CS101989		Calcium silicate		
	1	$t = 0 \rightarrow 1800$ s	0.02592	1035
		$t = 60 \rightarrow 1800$ s	0.02593	1034
		$t = 0 \rightarrow 1150$ s	0.02624	1010
		$t = 60 \rightarrow 1150$ s	0.02638	999
		$t = 120 \rightarrow 1150$ s	0.02628	1007
	2	$t = 200 \rightarrow 1800$ s	0.02584	1003
	3	$\bar{T} = 0.3 \rightarrow 0.5$	0.02505	1100
		$\bar{T} = 0.3 \rightarrow 0.4$	0.02490	
		$\bar{T} = 0.4 \rightarrow 0.5$	0.02302	
DOW90589		Polystyrene		
	1	$t = 0 \rightarrow 1800$ s	0.10380	1640
		$t = 60 \rightarrow 1800$ s	0.10605	1571
		$t = 0 \rightarrow 600$ s	0.09384	2010
		$t = 60 \rightarrow 600$ s	0.10240	1685
		$t = 120 \rightarrow 600$ s	0.10423	1627
	3	$\bar{T} = 0.3 \rightarrow 0.5$	0.10827	1359
		$\bar{T} = 0.3 \rightarrow 0.4$	0.10818	
		$\bar{T} = 0.4 \rightarrow 0.5$	0.10776	

not constant over the 0.3 to 0.5 range. As long as a consistent range is used, the analysis should be correct. This assumption has not been proved and could lead to some of the differences.

Finally, Fig. 7 shows calculated and measured temperature vs time curves. In all three cases illustrated, an approximately ±5% range in the C value predicted by Method 3 is

ORNL-DWG 17163

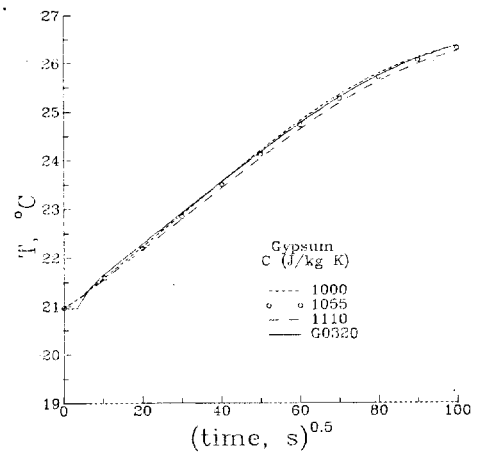

ORNL-DWG 17164

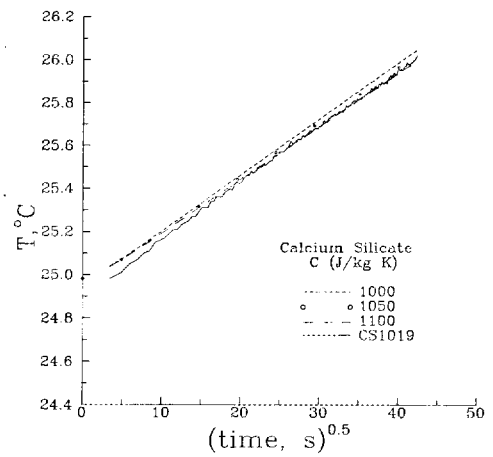

ORNL-DWG 17165

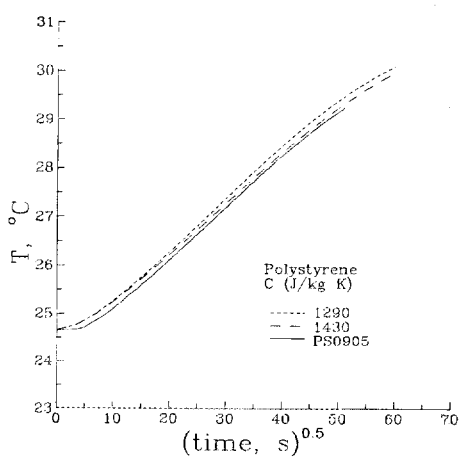

Fig. 7. Comparison of calculated and measured heater temperature changes for (a) gypsum (GOW), (b) calcium silicate (CS1), and (c) polystyrene.

shown. While there is clearly an offset in the absolute value of the temperature curve that results from the shift in C, it is not as clear that a significant change in the slope occurs. It is the slope that is important to Method 3. It is also clear that the "best" agreement occurs between dimensionless temperatures of 0.3 and 0.5, but not as good agreement occurs at short times.

Analysis to determine the sensitivity of this method is needed. This analysis should look at both sensitivity to C and errors in temperature measurement from data acquisition and conversion. Would other portions of the temperature response curve be better for determining C?

Radiation heat transfer in the less dense materials may also be important. This mechanism has not been incorporated into the current work. Materials with known specific heat are required to evaluate which method is correct.

5. TEST SPECIMENS

Two-sided and one-sided steady-state and two-sided transient tests were conducted on the building material specimens described in this section and listed in Table 7. The heater was positioned at the mid-plane of each test specimen, and the entire heater was covered by the specimen or by a perimeter material of similar properties.

5.1 GYPSUM BOARDS

The gypsum test specimen (GOW) was formed from a stack of eight boards (1.25 cm thick by 0.6 m by 0.9 m) cut from full-size gypsum wall boards (1.25 cm thick by 1.2 m by 2.4 m).[12] Test specimens containing about 15 (wt % wax (G15W) or about 30 wt % wax (G30W) were produced by immersing full-size gypsum wall boards for fixed times in a bath of molten wax held at 75°C. This procedure allowed the wax to suffuse into the pore spaces of the gypsum.[13] The full-size boards were cut to produce the 0.6- by 0.9-m specimen. Eight pieces of each material were stacked to produce a specimen approximately 10 cm thick for use in the UTHA. Table 7 provides the thicknesses and average densities for the three test specimens. Table 8 contains estimates of test specimen properties at 24°C using literature data for k and C for gypsum and wax. Three k-values[14,15] at 24°C for gypsum board predict an increase with density (ρ); this is described to 5% by the equation

Table 7. Building material test specimens for steady-state and transient tests in the Unguarded Thin-Heater Apparatus

			Test Specimen, m			
Code	Material	Density (kg/m^3)	Total thickness	Width	Length	Perimeter
GOW	Gypsum board	695.1	0.1002	0.6	0.9	GOW
G15W	Gypsum board - 14.1 wt % wax	816.9	0.1011	0.6	0.9	GOW
G30W	Gypsum board - 30 wt % wax	1000.0	0.1006	0.6	0.9	GOW
CS1	Calcium silicate 1	307.4	0.077	0.9	1.5	-
CS2	Calcium silicate 2	443.9	0.077	0.9	1.5	-
CS3	Calcium silicate 3	605.1	0.077	0.9	1.5	-
WSF	White spruce flooring	451.5	0.097	0.9	1.5	WSF
DFP	Douglas fir plywood	500.9	0.073	0.9	1.5	DFP
SYPF	Southern yellow pine flooring	575.2	0.098	0.9	1.5	SYPF
PS	Polystyrene (HCFC-142b) age: 25 d 45 d 74 d 127 d 227 d	30.0	0.101	0.9	1.5	-
CFC	Polyisocyanurate (CFC-11)	30.2	0.064	0.9	1.5	-

$$k\ (W/m \cdot K) = -1.741 \cdot 10^{-2} + 2.2914 \cdot 10^{-4}\ \rho\ (kg/m^3)\ . \tag{13}$$

Data were not found that gave the temperature dependence of k of gypsum boards.

The C of gypsum ($CaS0_4 \bullet 2\ H_20$, ρ theoretical density 2320 kg/m^3) has been measured[16, 17] from 18 to 303 K. Seventeen individual data points[18] tabulated from 240 to 303 K are described to 1% by the equation

$$C\ (J/kg \cdot K) = 377.8 + 2.36258\ T\ (K)\ . \tag{14}$$

Table 8. Estimated properties at 24°C for gypsum-wax test specimens

Estimated properties	GOW	G15W[(a)]	G30W
k, W/m•K	0.1614	0.1614	0.1943
C, J/kg•K	1079.0	1262.0	1465.0
α, m^2/s•10^7[b]	1.892	1.595	1.326

[a]Actual composition was 14.1 wt % wax.

[b]α is 1.892×10^{-7} m^2/s for GOW.

Measured k-values[19] for solid wax (n-octadecane) between 3 and 15°C are described to 1% by the equation

$$k\ (W/m \cdot K) = 0.3433 - 0.00168\ t\ (°C)\ . \tag{15}$$

Data were not found that describe the k of liquid n-octadecane.

The C of liquid n-octadecane was estimated to be 2364 J/kg•K at 24°C using a corresponding states model.[20] The density of wax was 770 kg/m^3 (ref. 19).

The Eucken equation[21] for two-phase materials was used to calculate k of the specimens

$$k_m = k_1 \frac{1 - f + f[3k_2/(2k_1 + k_2)]}{1 - f + f[3k_1/(2k_1 + k_2)]}\ , \tag{16}$$

where k_m is the conductivity of the two phase material,

k_1 is the conductivity of the continuous phase,

k_2 is the conductivity of the discontinuous phase (wax) and,

f is the volume fraction of the discontinuous phase (wax).

Published data for C were used to calculate C for the specimens from the rule of mixtures. With increasing wax content the predicted k and C increase, but the predicted thermal diffusivity (α) decreases. Separate steady-state and transient tests were run on the three specimens listed in Table 7. In each test the 0.6- by 0.9-m specimens were surrounded by a perimeter of GOW to cover the 0.9- by 1.5-m heater. Thermocouples were added at the midpoints of each side of the specimen stack, and sheets of 0.07-mm-thick polyethylene were inserted at the four screen-specimen and plate-specimen interfaces to avoid possible bonding between specimens, the plates, and the screen.

5.2 CALCIUM SILICATE BOARDS

The calcium silicate board test specimens were duplicate slabs, each nominally 0.9 by 1.5 by 0.038 m, of three densities (307, 444, and 605 kg/m^3) that were conditioned in the Building Materials laboratory prior to testing.[22] Calcium silicate insulation is a reacted hydrous calcium silicate material made using uncalcined diatomaceous earth and lime blended with reinforcing fibers. The insulation is recommended for use for temperatures from 100 to 1200°F inclusive.[23] The insulation is not $CaO \cdot SiO_2$, and while there is no exact chemical formula for hydrous calcium silicate, it is near $Ca_6Si_6O_{17}(OH)_2$. Table 9 contains k (24°C) values as a function of density that were obtained from ASTM standards and literature on calcium silicate. Figure 8 shows that the k-values in Table 9 increase with density, and the values show a separation of about 0.022 W/m•K (0.15 Btuin./h•ft^2•°F) at 240 kg/m^3 (15 lb/ft^3). The first five materials with higher k-values are described to 1% by

$$k = 0.09079 - 1.1795 \cdot 10^{-4} \rho + 2.7675 \cdot 10^{-7} \rho^2, \ (240 < \rho < 1050) \ . \tag{17}$$

Items 6–9 with lower k-values average 0.056 W/m•K (0.388 Btu•in./h•ft^2•°F).

Specific heat values of 836–878 J/kg•K and 1045–1170 J/kg•K are listed for hydrous calcium silicate.[14] Use of a C value of 1000 J/kg•K and Eq. (17) yields the estimated properties given in Table 10 for the calcium silicate specimens. This tabulation shows that the estimated thermal diffusivity decreases as the specimen density increases.

Calcium silicate boards of two densities (449 kg/m^3 and 641 kg/m^3) have been tested at PABCO and NIST (Boulder) from 40 to 540°C in high-temperature guarded hot plate apparatuses. The results at 40°C (Table 9) show that the PABCO results are 10 and 33%

Table 9. Thermal conductivity values at 24°C as a function of density for calcium silicate insulation

Item	Density		k (25°F)		Comment	Reference
	lb/ft^3	kg/m^3	Btu•in./h•ft^2•°F	W/m•K		
1	15	240	0.54	0.0779	Type II, fitted	14
2	15	240	0.545	0.0786	Type II, fitted	24
3	26	417	0.628	0.0906	Class A, fitted	25
4	38	609	0.838	0.121	Class B, fitted	25
5	65	1041	1.856	0.268	Class C, fitted	25
6	12.8	205	0.382	0.0551		26
7	13.1	210	0.376	0.0542		27
8	14	224	0.40	0.0577		14
9	15	240	0.39	0.0562		24
10[a]	19.2	308	0.453	0.0653		
11[a]	27.7	444	0.517	0.0746		
12[a]	37.8	605	0.616	0.0889		
13[b]	28.0	449	0.580	0.0836		PABCO
14[b]	28.0	449	0.527	0.0760		NIST (B)
15[b]	40.0	641	0.69	0.0995		PABCO
16[b]	40.0	641	0.524	0.0756		NIST (B)

[a]This research Sect. 6.12.
[b]k-values at °C.

ORNL-DWG BMG90-1

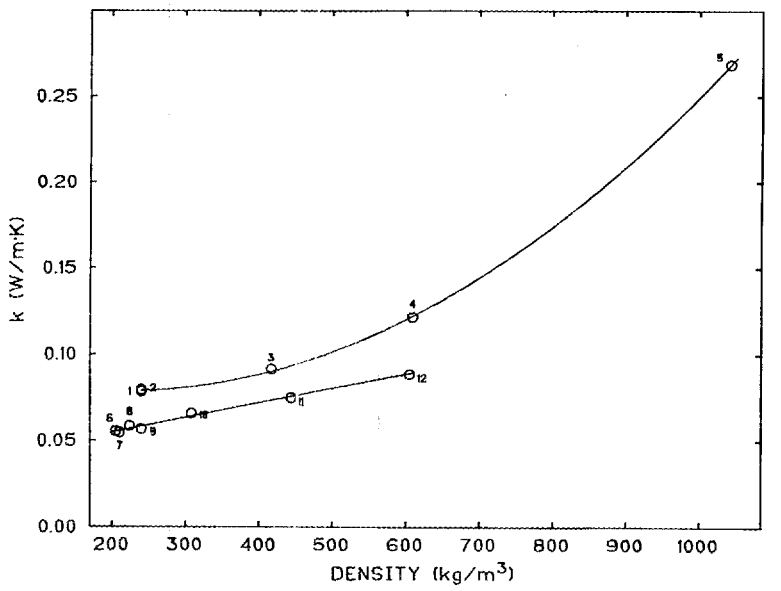

Fig. 8. Thermal conductivity at 24°C of calcium silicate as a function of specimen density (see Table 9).

Table 10. Estimated properties at 24°C for calcium silicate boards

Estimated property density (kg/m^3)	CS1 308	CS2 444	CS3 605
k, W/m•K	0.0807	0.0930	0.1207
C, J/kg•K	1000.0	1000.0	1000.0
α m^2/s•10^7[a]	2.62	2.09	2.00

[a]α is 2.62 x 10^{-7} m^2/s for CS1.

greater than the NIST (B) results. The PABCO results increase with density, but the NIST (B) results do not. The UTHA tests were conducted to help resolve these significant differences.

5.3 WOOD PRODUCTS

The southern yellow pine flooring and white spruce flooring test specimens were made by gluing individual tongue-and-groove boards together and planing their surfaces to produce

0.9- by 1.5-m slabs of uniform thickness. The Douglas fir plywood test specimen was made from 1.2- by 2.5-m plywood boardstock by cutting a 0.9- by 1.5-m slab and sanding one surface to produce a uniform thickness. A center 0.6- by 0.6-m^2 section was cut from each to break the conduction path in each slab. Three slabs were stacked on each side of the heater to yield a six-slab test specimen with the heater sandwiched at the stack centerline. Additional thermocouples were added at the board interfaces. Tests were conducted with heat flowing perpendicular to the board face, as would be the case for a flooring application.[28]

Test specimens were conditioned in the Building Materials laboratory for several weeks prior to testing, and the average moisture content did not change significantly as a result of the thermal tests. Table 11 gives the average pre- and post-test moisture contents. These values were determined using a Model RDM-1 Portable Resistance Meter made by Delmhorst Instrument Company, Towaco, New Jersey. Some moisture redistribution from warm to cold regions was noted.

Table 11. Average moisture contents of wood-product test specimen (wt %)

			Board		(Heater)[a]		Board	
		Average	1	2	3	4	5	6
White spruce flooring	Pre-test	11.1	11.0	11.4	11.1	11.0	11.1	10.8
	Post-test	11.8	13.7	12.1	9.6	10.1	11.9	13.3
Douglas fir plywood	Pre-test	9.4	10.5	8.6	8.8	9.8	9.3	9.6
	Post-test	8.6	10.2	8.2	7.6	7.8	8.3	9.5
Southern yellow pine flooring	Pre-test	8.6	8.5	8.6	8.6	9.4	8.5	8.1
	Post-test	8.9	10.4	8.6	7.7	8.5	9.1	9.1

[a]The thin heater was positioned between Boards 3 and 4.

Available information on the thermal conductivity and specific heat of wood and wood products was assessed by A. TenWolde, J. D. McNatt, and L. Krahn.[29] They present equations to predict k and C as a function of density and moisture content:

$$k(wood) = \frac{D}{1000}\,(0.1941 + 0.004064\,M) + 0.01864 \tag{18}$$

$$k\,(plywood) = 0.86\,k\,(wood) \tag{19}$$

$$C_o\,(dry) = 0.003867\ T + 0.1031,\ kJ/kg{\cdot}K \tag{20}$$

$$C\,(moist) = \frac{C_o + 0.01\ MCw}{1 + 0.01\ M} + A\ , \tag{21}$$

where M is the moisture content (percent),

Cw is the C of water (4.186 kJ/kg•K),

A is a correction term.

$$A = (0.0002355\,T - 0.0001326\,M - 0.06191)\ M\ . \tag{22}$$

Equations (18)-(22) were used to estimate the properties of the three wood product test specimens (Table 12). This tabulation shows for the woods that a 37% increase in density yields an estimated increase in k of 19%, a decrease in C of 5%, and a 1% decrease in α.

Table 12. Estimated properties at 24°C for wood-product test specimen

	White spruce flooring		Douglas fir plywood		Southern yellow pine	
Density, kg/m^3	452		501		575	
Moisture content, wt %	0	11.5	0.0	9.0	0.0	8.8
Estimated property						
k, W/m•K	0.106	0.127	0.0995	0.1152	0.1306	0.1513
C, J/kg•K	1251.6	1627.3	1251.6	1554.1	1251.6	1548.1
α, m^2/s•10^7[a]	1.87	1.73	1.59	1.48	1.81	1.69

[a] α is 1.87 x 10^{-7} m^2/s for white spruce flooring.

5.4 PLASTIC CELLULAR FOAMS

Thermal test specimens, 0.9 by 1.5 m, were prepared from 1.2- by 2.4-m boardstock of extruded polystyrene and polyisocyanurate plastic cellular foam.[31] Each polystyrene test specimen was nominally 0.051 m thick, had a density of 30 kg/m^3, and was tested with the as-produced surfaces.[30] The polystyrene was foamed with HCFC-142b. The polyisocyanurate test specimen was prepared by planing a rigid foam boardstock blown with CFC-11 that was nominally 0.038 m thick and faced with a 0.6- by 10^{-3}-m (0.025-in.) GAF paper facer.[32] The density of the test specimen was 30.2 kg/m^3, and each specimen was nominally 0.032 m thick.

Typical thermal properties given by Strzepek[32] for extruded polystyrene are k(initial), 0.020 W/m•K; k (after 100 days), 0.0288 W/m•K; and a range of C values from 1130 to 1300 J/kg•K. Those by Strzepek[32] for polyisocyanurate are k (initial), 0.017 W/m•K; k(beyond 1 year), 0.024 W/m•K; and a range of C from 840 to 1050 J/kg•K. Sparks[33] provides k-values for both materials (32 kg/m^3) that agree with those of Strzepek and C values at 300 K of 1150 J/kg•K for polystyrene and 1525 J/kg•K for polyisocyanurate (49 kg/m^3). The latter value was measured by Luikov et al.[34] from 10 to 400 K. These values were used to estimate the properties of the test specimens given in Table 13. The estimated α for both increase with time, and the value for extruded polystyrene is about 60% greater than that of the polyisocyanurate foam.

Table 13. Estimated properties at 24°C for plastic cellular foam test specimens

	Extruded polystyrene		Polyisocyanurate	
Density, kg/m^3	30		30.2	
Estimated property	Initial	After 100 days	Initial	After 1 year
k, W/m•K	0.020	0.0288	0.017	0.024
C, J/kg•K	1150		1525	
α, m^2/s•10^7[a]	5.8	8.3	3.7	5.2

[a] α is 5.8 x 10^{-7} m^2/s for extruded polystyrene.

6. TEST RESULTS

Subsection 6.1 describes the k-values as a function of temperature that were determined for the building material test specimens from steady-state tests and those determined before and at the end of transient tests. Subsection 6.2 describes the results obtained by analyzing the transient data for the building material test specimens. The transient analysis yielded $k\rho C$ and used the measured k-values to obtain C as a function of temperature.

6.1 STEADY-STATE THERMAL CONDUCTIVITY VALUES

6.1.1 Gypsum Boards

Table 14 contains the k-values as a function of temperature for test specimens GOW, G15W, and G30W. For example, T2, 0.3 is the k-value obtained from 300 s of data before

Table 14. Summary of *k*-values for GOW, G15W, and G30W test specimens

Data point	Mean temperature (°C)	*k* (W/m•K)	t(hot), t(cold) (°C)	Data point	Mean temperature (°C)	*k* (W/m•K)	t(hot), t(cold) (°C)
GOW test specimen							
D1	23.99	0.1766	27, 21	T1, 1.8	24.00	0.1786	27, 21
				T2, 0.3	24.02	0.1793	27, 21
D2	26.58	0.1765	32, 21	T2, 1.8	27.27	0.1785	32, 22
				T3, 0.3	27.31	0.1788	32, 22
D4	44.72	0.1762	52, 37	T3, 1.8	30.15	0.1782	38, 22
				T4, 0.3	30.14	0.1782	38, 22
				T1R, 1.8	24.02	0.1787	27, 21
Average		0.1764				0.1786	
G15W test specimen							
D1	22.93	0.2019	23, 22	T1, 1.8	22.90	0.2010	23, 22
D2	25.68	0.1952	29, 23	T2, 1.8	25.65	0.1952	29, 22
D3	29.75	0.1918	33, 27	T3, 1.8	29.27	0.1920	33, 27
D4	33.85	0.1918	41, 27	T4R, 1.8	29.76	0.1921	33, 27
D4R	33.88	0.1917	41, 27	T4R, 1.8	33.83	0.1917	41, 27
D5	29.79	0.1922	33, 27	T6, 0.3	33.84	0.1918	41, 27
Average D3-D5		0.1919		T3 - T6		0.1919	
G30W test specimen							
D1	23.03	0.2342	24, 22	T5A, 1.8	24.75	0.2400	27, 22
				T5B, 0.3	24.78	0.2424	27, 22
D2	29.21	0.2322	32, 27	T5B, 1.8	28.25	0.2369	34, 22
				T5C, 0.3	28.25	0.2369	34, 22
D3	32.55	0.2322	38, 27	T5D, 1.8	25.04	0.2412	28, 23
				T5E, 0.3	25.03	0.2410	28, 23
				T6, 1.8	29.14	0.2316	32, 27
				T7, 0.3	29.16	0.2333	32, 27
				T7, 1.8	32.43	0.2330	38, 27
				T8, 0.3	32.54	0.2326	38, 27
Average D2-D3		0.2322		T6 - T8		0.2326	

transient T2; and T2, 1.8 is that obtained from 1800 s of data at the end of transient T2. Table 14 contains the nominal temperatures of the hot and cold surfaces for each test.

The k-values for GOW specimen are within 1% of the average, 0.1786 W/m•K, and are independent of temperature from 24 to 45°C (Fig. 9).

The eight k-values for G15W specimen obtained with the cold surface near 27°C are within 0.2% of the average, 0.1919 W/m•K, are independent of temperature from 29 to 34°C, and are greater than k of GOW by about 8%. The two k-values obtained with the cold surface near 22°C and a small temperature difference across the specimen are within 0.5% of their average of 0.2014 W/m•K. The fraction of wax that is solid is unknown. However, this result suggests that the k of the G15W composite with solid wax exceeds that with liquid wax by about 5% and exceeds k (GOW) by about 13%.

The six k-values for G30W specimen obtained with the cold surface near 27°C are within 0.7% of their average, 0.2325 W/m•K, are independent of temperature, and are greater than

ORNL-DWG 17166

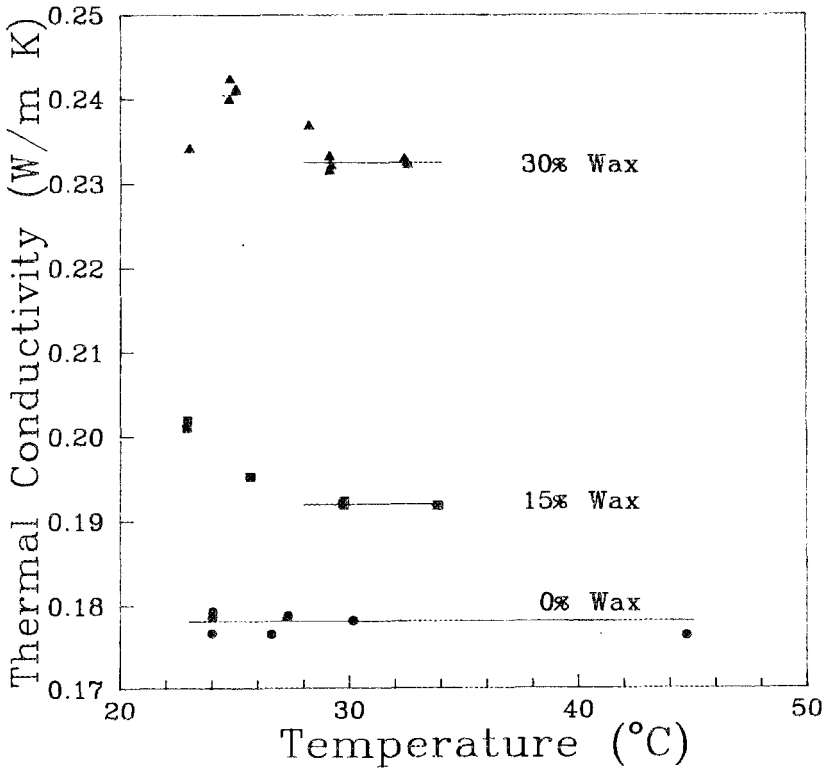

Fig. 9. Thermal conductivity as a function of temperature for gypsum-wax specimens.

near 22°C are within 3.5% of their average, 0.2389 W/m•K. This result suggests that the k of the composite with solid wax exceeds that with liquid wax by about 3% and that of GOW by about 35%.

The average k-value for GOW is 25% greater than the estimated value in Table 8. This value and the data in ref. 14 are described to 2% by

$$k(W/m \cdot K,\ 24°C) = 0.1076 + 9.8344 \times 10^{-5}\ \rho\,(kg/m^3)\ . \tag{23}$$

This equation predicts k-values that are about 17% greater than those given in ref. 15. The k-value for GOW was used with Eqs. (15) and (16) to predict the k-values at 24°C for the G15W and G30W composites respectively. The predicted composite k-values were 0.1944 and 0.2208 W/m•K; these are 3.5 and 8% above the average measured k-values for G15W and G30W respectively.

6.1.2 Calcium Silicate Boards

Table 15 contains the measured k-values as a function of temperature for test specimens CS1, CS2, and CS3. The k-values increase with temperature and density. The individual

Table 15. Thermal conductivity values for three calcium silicate specimens as measured in the Oak Ridge National Laboratory unguarded thin-heater apparatus

	Mean temperature (°C)	k (W/m•K)
CS1, 307 kg/m³	25.99	0.06586
	27.74	0.06562
	31.16	0.06562
	35.94	0.06587
	40.95	0.06623
	52.66	0.06723
	58.36	0.06765
$k = 6.3842 \times 10^{-2} + 6.3009 \times 10^{-5}\ t$, ±0.26%[a]		
CS2, 444 kg/M³	27.36	0.07473
	35.50	0.07559
	41.28	0.07597
	53.21	0.07686
	59.29	0.07736
$k = 7.2640 \times 10^{-2} + 7.9893 \times 10^{-5}\ t$, ±0.077%		
CS3, 605 kg/m³	27.08	0.08940
	33.24	0.08953
	38.00	0.08977
	52.58	0.09119
	57.97	0.09179
$k = 8.7021 \times 10^{-2} + 7.9729 \times 10^{-5}\ t$, ±0.20%		

[a]Average deviation.

specimen data were fitted by a least-squares method to a linear function of temperature. Table 15 contains the coefficients obtained and shows that the average deviation of the results from the equations is less than 0.25%. These linear equations were used to obtain the k (24°C) values indicated in Table 9 as items 10, 11, and 12. These values and items 6, 7, 8, and 9 are described by a nonlinear equation with an average deviation of less than 2%:

$$k = 0.03620 + 9.2316 \times 10^{-5}\,\rho - 9.505 \times 10^{-9}\,\rho^2 \,. \tag{24}$$

Figure 10 is a plot of the k-values as a function of temperature for these three specimens and test results from PABCO and NIST (Boulder) on specimens of densities of 449 kg/m^3 and

ORNL-DWG BMG90-3

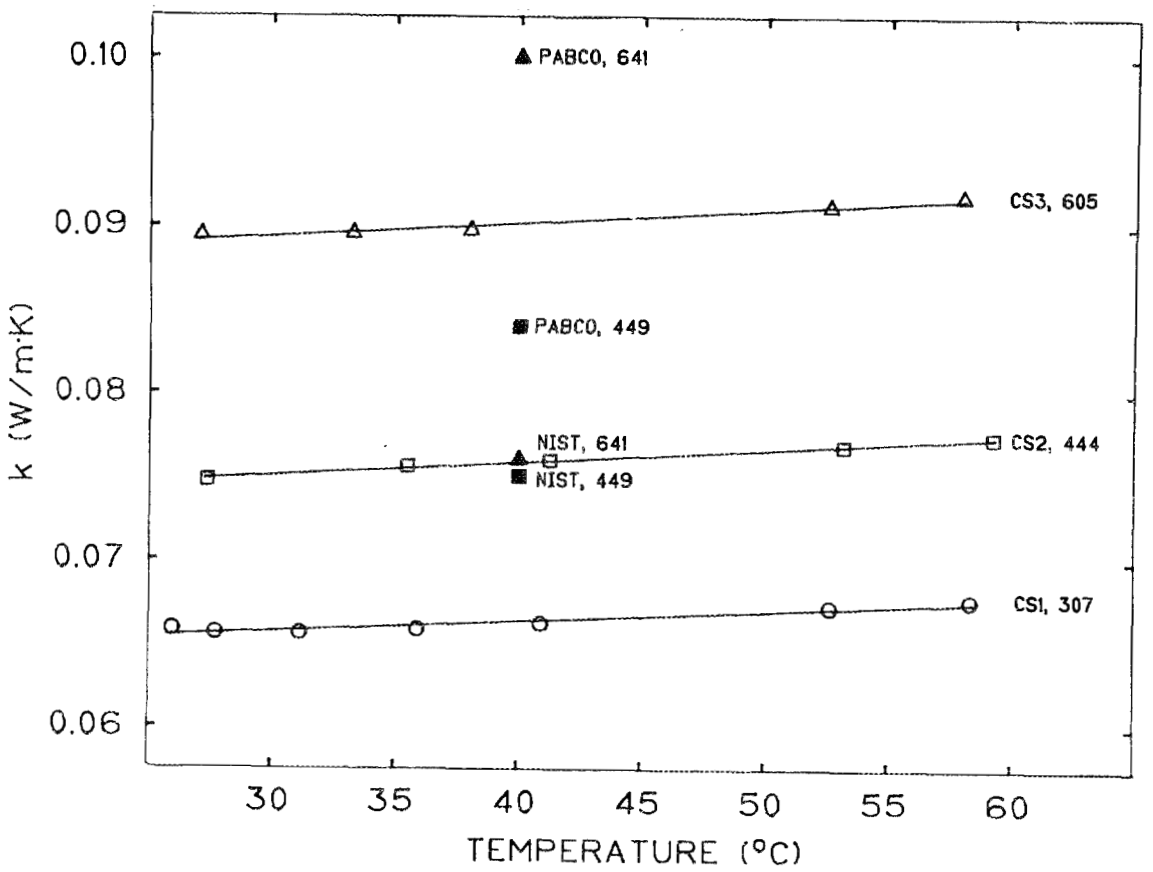

Fig. 10. Thermal conductivity of three calcium silicate specimens as a function of temperature.

641 kg/m^3. The ORNL and NIST results agree to 1% for the specimen with a density of 449 kg/m^3. The PABCO results are about 10% higher than these two data sets. The ORNL results are about 19% higher than the NIST results and about 9% lower than the PABCO results on the 605- kg/m^3 specimen.

6.1.3 Wood Products

The k results obtained on the southern yellow pine flooring (SYPF), white spruce flooring (WSF), and Douglas fir plywood (DFP) test specimens are given in Table 16. The k-values increase with temperature for the three products, and the WSF and DFP k-values are nearly equal and less than that of the SYPF test specimen. The individual specimen data were fitted by a least-squares method to a linear function of temperature. Table 16 contains the resulting equations and shows that the average deviation of the results from the equations is less than 0.3% Figure 11 is a plot of k-values as a function of temperature for these three products and includes the estimated k-values at 24°C for dry and moist specimens given in Table 11. The measured k-values at 24°C are within 3% of the estimated k-values for 0% moisture content: WSF (2.9%), DFP (2.2%), and SYPF (2.5%). However, the measured k-values at 24°C are significantly lower than the estimated k-values for the measured moisture content of the test specimens: WSF (-19%), DFP(-11.7%), and SYPF (-15.9%). If this trend is found for the other specimens available from the Forest Products Laboratory, it suggests that the equations used to estimate the k-values should be modified.

Table 16. Thermal conductivity values for three wood products

	Mean temperature (°C)	k (W/m•K)
WSF	24.05	0.1030
	28.18	0.1037
	35.53	0.1046
	43.34	0.1054
	47.63	0.1073
	47.73	0.1064
$k = 0.09920 + 1.5537 \times 10^{-4}\, t$, ±0.28%[a]		
DFP	23.60	0.1014
	27.24	0.1026
	32.43	0.1030
	35.02	0.1034
$k = 0.09786 + 1.6039 \times 10^{-4}\, t$, ±0.18%		
SYPF	23.71	0.1274
	27.12	0.1277
	32.95	0.1285
	45.89	0.1309
$k = 0.1234 + 1.6153 \times 10^{-4}\, t$, ±0.11%		

[a]Average deviation.

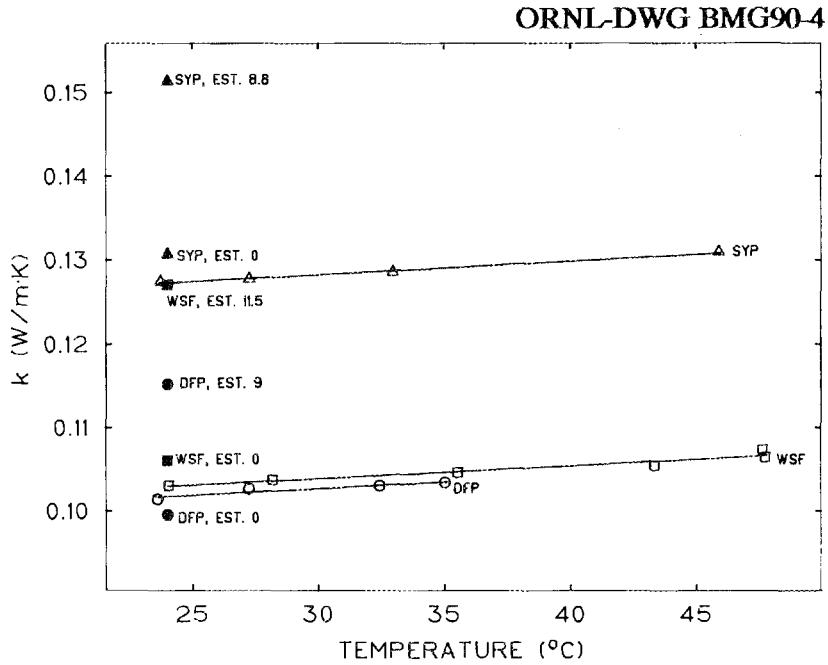

Fig. 11. Thermal conductivity of three wood-product test specimens as a function of temperature.

One reason for doing these tests was to establish the temperature dependency of k of typical wood products, as recommended by A. TenWolde, et al.[29] The average percent deviation of the least-squares fits is quite low. The slope terms for the three products agree to ±2%. The increase in k from 20 to 50°C is 3.83%, or about 0.13% per degree centigrade. This increase is less than half of the 10% per 50°C increase in temperature cited by A. TenWolde, et al.[29]

6.1.4 Plastic Cellular Foams

Table 17 lists the k-values for extruded polystyrene foamed with HCFC 142b as a function of temperature and time after manufacture. Table 17 includes results on the polyisocyanurate cellular test specimen foamed with CFC-11 and tested 398 d after manufacture. This test specimen will be circulated to four laboratories to compare results obtained using 0.6- by 0.6-m comparative heat flow apparatuses. Table 17 contains the equations obtained by a least-squares method of fitting the data to a linear function of temperature. The average percent deviation is less than ±0.15% for the five data sets for the extruded polystyrene test specimen and is ±0.3% for the polyisocyanurate test specimen.

Table 17. Thermal conductivity values as a function of temperature and time after production for extruded polystyrene foamed with HCFC 142b and polyisocyanurate foamed with CFC-11

Specimen: age	Mean temperature (°C)	k (W/m•K)
PS (HCFC-142b): 25 d	27.90	0.02624
	33.50	0.02685
	47.54	0.02858
HF (up)	27.85	0.02634
HF (down)	27.84	0.02627
$k = 0.02302 + 1.1650 \times 10^{-4}\, t$, ±0.15%[a]		
PS (HCFC-142b): 45 d[b]	27.80	0.02719
	33.18	0.02786
	42.95	0.02910
$k = 0.02368 + 1.2618 \times 10^{-4}\, t$, ±0.014%		
PS (HCFC-142b): 74 d	27.72	0.02811
	32.96	0.02867
	46.60	0.03033
$k = 0.02480 + 1.1841 \times 10^{-4}\, t$, ±0.081%		
PS (HCFC-142b): 131 d[b]	27.48	0.02895
	32.58	0.02949
	43.14	0.03079
$k = 0.02567 + 1.1831 \times 10^{-4}\, t$, ±0.085%		
PS (HCFC-142b): 227 d[b]	27.47	0.02937
	32.47	0.02997
	42.92	0.03125
$k = 0.02602 + 1.2181 \times 10^{-4}\, t$, ±0.012%		
PIR (CFC-11): 398 d[b]	27.31	0.02068
	39.98	0.02191
	50.14	0.02295
HF (up)	39.83	0.02196
HF (down)	39.96	0.02174
$k = 0.01794 + 9.9054 \times 10^{-5}\, t$, ±0.29%		

[a]Average deviation.
[b]Transient tests were conducted at these times.

Figure 12 shows that the k-values increase with temperature and increase with time after manufacture for the extruded polystyrene test specimen. For the polyisocyanurate specimen,

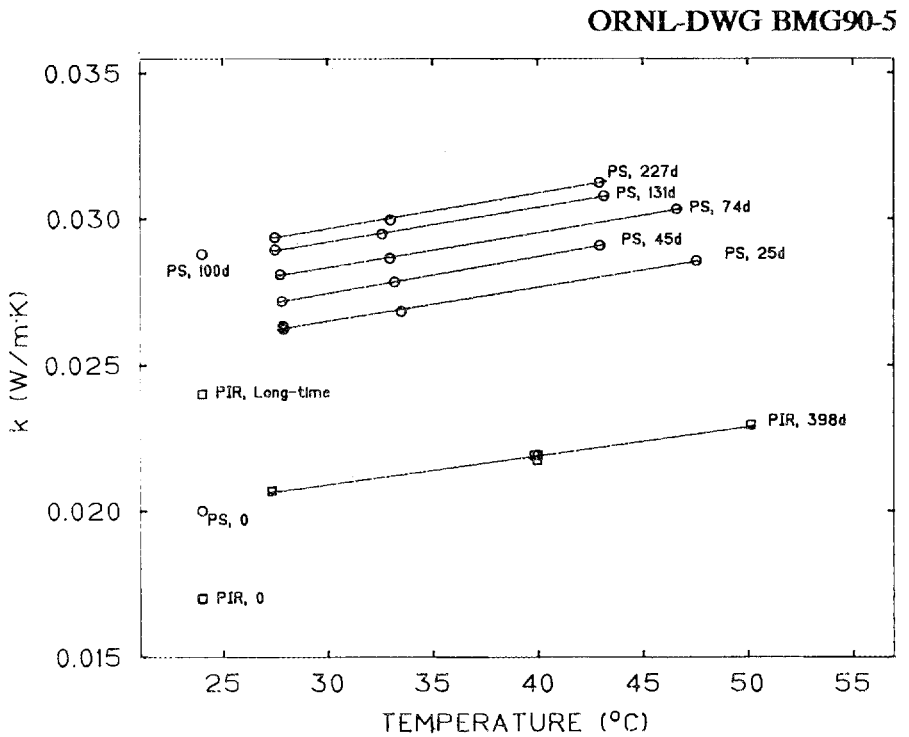

Fig. 12. Thermal conductivity as a function of temperature and time after manufacture for extruded polystyrene (HCFC-142b) and polyisocyanurate (CFC-11).

398 d after manufacture the k-values increase with temperature. The slope terms for the extruded polystyrene agree to ±4.2% and have an average value of 1.202×10^{-4} °C^{-1}. The polyisocyanurate test specimen has a slope term that is about 18% below this average slope.

The equations given in Table 16 for extruded polystyrene were used to obtain the values of k at 24°C, and these values are plotted as a function of time after manufacture in Fig. 13. These data were fitted by a least-squares method to ±0.4% by

$$k = 0.02492 + 4.317 \times 10^{-5}\, t - 1.127 \times 10^{-7}\, t^2, \quad t{:}d\ . \tag{25}$$

Equation (25) is only valid for interpolating within these data and should not be extrapolated to longer times. The initial k (24°C) value, 0.02492, is about 25% greater than the initial value estimated in Table 13, but the 100-day value, 0.0281, is within 3% of the estimated 100-day value. The k (24°C) value for the polyisocyanurate test specimen is within the predicted range.

ORNL-DWG BMG90-6

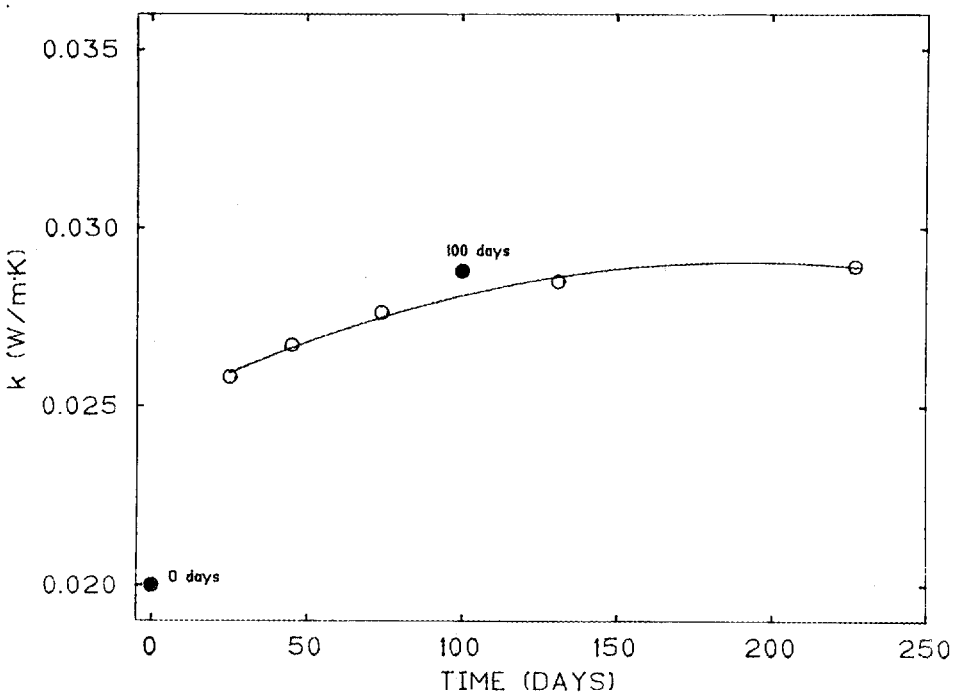

Fig. 13. Thermal conductivity at 24°C of extruded polystyrene (HCFC-142b) as a function of time after manufacture.

In a study on the aging of thin specimens planed from polyisocyanurate roof insulation boards,[35] we have noted that the time dependency of k can be scaled usefully by $\ln 100\,k$ vs $(\text{time})^{1/2}/\text{thickness}$. This test procedure provides a means to measure the two-stage diffusion process that causes foams with permeable facers or no facing to slowly lose their insulating power as a function of time. Without a barrier, air diffuses into the foam cells, and the blowing agent diffuses out of the foam cells. This process changes the cell gas composition, which changes the cell gas thermal conductivity, which changes the product's thermal resistance.

If one empirically assumes that k can be described by an exponential dependence on diffusion coefficient (D), time (t), and thickness (h),

$$k = k_0 \exp\{(Dt)^{1/2}/h\} , \tag{26}$$

where k_0 is the initial thermal conductivity, then one observes

$$\ln k = \ln k_0 + (Dt)^{1/2}/h \text{ and} \tag{27}$$

$$Y = A + B\,X, \tag{28}$$

where $A = \ln k_0$,

$Y = \ln k$,

$X = t^{1/2}/h$,

$B = D^{1/2}$.

Thus, if one measures the k of a foam product of thickness (h) as a function of aging time (t), then a plot of Y vs X should yield a straight line with slope B. A least-square fitting of the data to the straight line represented by Eq. (28) yields an intercept of $\ln k_0$ and a slope of $D^{1/2}$.

Leon Glicksman of the Massachusetts Institute of Technology (MIT) has provided results[36] of calculations from a model for aging of plastic foam insulations. His results produce two linear regions when scaled to (time)$^{1/2}$/thickness (i.e., an initial linear region associated with inward diffusion of air components and a second linear region associated with outward diffusion of chlorofluorocarbon gas). For his calculations the linear regions intersect at a value of about 0.3 (d)$^{1/2}$/mm and show a transition region from about 0.2 to 0.5 (d)$^{1/2}$/mm.

We have applied the above treatment to the five k (24°C) values with a thickness of 50.8 mm (2 in.). The results (Fig. 14) show a linear behavior for the first three data points.

ORNL-DWG BMG90-42

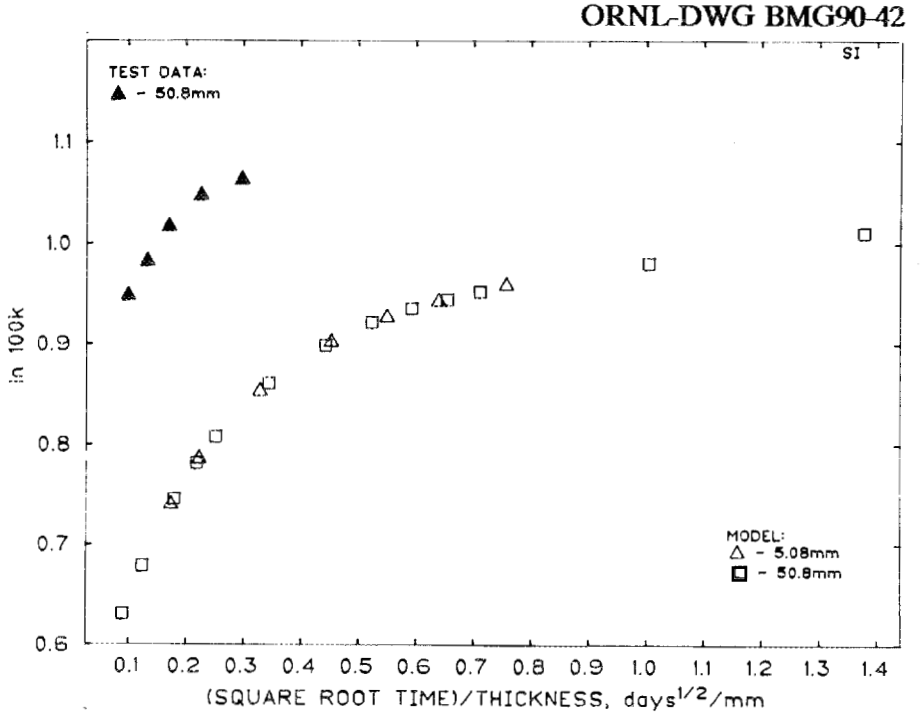

Fig. 14. Natural logarithm of 100 k vs (time)$^{1/2}$/thickness for the Massachusetts Institute of Technology model of aging by a plastic foam and Oak Ridge National Laboratory data on extruded polystyrene.

The fourth and fifth points do not fall on the same linear relation; this indicates that a transition to the second linear region is occurring.

The linear regions for the MIT model calculations are described by

$$\ln 100\,k = 2.454 + (18.78 \times 10^{-8}\,t)^{1/2}/h \text{ and} \tag{29}$$

$$\ln 100\,k = 2.826 + (9.23 \times 10^{-10}\,t)^{1/2}/h, \tag{30}$$

where t is time in seconds and h is thickness in centimeters. The three extruded polystyrene data points are described by

$$\ln 100\,k = 2.7896 + (10.81 \times 10^{-8}\,t)^{1/2}/h, \tag{31}$$

where h is 5.08 cm. The coefficients for the time variable have the units of square centimeters per second and represent apparent diffusion coefficients. For Eqs. (29) and (30) the ratio of these coefficients is about 200. This ratio is the correct order of magnitude expected for air components and CFC-11 gas. For Eqs. (29) and (31) the coefficients differ by less than a factor of 2, as might by expected for air components in two types of plastic foam. The intercept of Eq. (31) corresponds to the initial k (24°C) and has a value of 0.02347 W/m•K, which is 2.5% lower than the prediction of Eq. (25).

6.2 TRANSIENT DATA ANALYSIS RESULTS

This section presents the results of analyzing the transient temperature response of the thin heater. Several methods of analysis have been described (see Subsects. 4.1, 4.2, and 4.3), and the results of applying these are described for each material. A comparison of applying Method 1 and Method 3 is given to show the differences in these two approaches.

Method 3, an iterative technique described in Subsect. 4.3, was employed to determine the specific heat values for all of the materials tested. The thermal conductivities measured by the steady-state technique (presented in Subsect. 6.1) and the densities and sample thicknesses (presented in Table 7) were used in the analyses. Table 18 lists the results of these calculations to obtain specific heat values. These differences are discussed in each material section.

6.2.1 Gypsum Boards Containing Wax

Table 19 lists the results obtained by analyzing the transient data for the GOW, G15W, and G30W specimens using Eqs. (4) and (5), Method 1.1. Each specimen was subjected to positive and negative step-changes in heat flux. The slope was determined from data that

Table 18. Specific heat values obtained by Methods 1 (1.1, 1.2) or 2, and 3

Material (TMR)	Temperature (°C)	C-M3 (J/kg•K)	C-M1 or M2 (J/kg•K)
	Gypsum		
GOW (0.0075)	23.3	1089	1048
	29.3	1121	1056
	34.8	1136	1078
	31.0	1115	1092
	23.6	1111	1055
G15W (0.0055)	22.8	3021	2461
	23.9	2923	2098
	29.0	1428	1425
	36.1	1301	1296
	35.2	1295	1274
G30W (0.0038)	23.9	7155	4116
	30.1	9336	5891
	29.2	1549	1534
	24.5	9270	6012
	25.0	4507[a]	1942
	28.6	1503	1528
	34.3	1502	1520
	33.6	1491	1526
	Calcium Silicate		
CS-1 (0.0231)	25.8	1100	1003
	28.3	1065	1005
	33.1	1050	1026
	41.0	1101	1050
	50.8	1123	1069
	43.9	1061	1021
CS-2 (0.0164)	26.8	1008	1027
	36.2	1074	1052
	50.5	1120	1078
	44.3	1024	1008
CS-3 (0.0121)	26.6	1041	1028
	34.0	1070	1052
	45.5	1094	1075
	40.4	1004	1000

Table 18. (Continued)

	Wood		
WSF (0.00777)	23.7	1672	1656
	28.8	1704	1668
	39.5	1748	1712
	37.3	1720	1723
DFP (0.0105)	23.3	1438	1400
	31.8	1487	1411
	44.2	1533	1421
	35.8	1492	1412
SYPF (0.0065)	23.4	1544	1576
	27.6	1596	1642
	36.3	1600	1676
	34.9	1601	1669
	Plastic		
PIR + CFC-11 (0.237)	26.7	1218	1530[b]
	40.0	1327	1640[b]
	43.6	1300	1680[b]
PS @ 45 d (0.132)	27.2	1359	12501[b]
	35.2	1397	1309[b]
	49.7	1552	1441[b]
	46.5	1485	1381[b]
PS @ 127 d (0.144)	26.9	1275	1157[b]
	34.4	1323	1226[b]
	49.0	1349	1239[b]
	46.8	1364	1283[b]
PS @ 227 d (0.145)	27.1	1308	1168[b]
	34.2	1270	1165[b]
	48.7	1350	1245[b]
	46.6	1353	1266[b]

[a]Based on slope for T equal 0.3 to 0.4.
[b]C-M2.

Table 19. Summary of specific heat (C) values from analysis of transient tests of gypsum-wax composites using Method 1.1

Transient test	Average temperature (°C)	Specific heat (J/kg•K)	Power change (W)	Slope (°C/(s)$^{1/2}$•10^2)	k•C (W^2/m•kg•K^2)	Transient range t(start, end, plate) (°C)
GOW: density, 694.5 kg/m^3; k, 0.178 W/m•K						
T1	22.85	1048	23.00	6.466	186.62	21, 27, 21
T2	28.54	1056	19.32	5.412	188.02	27, 33, 22
T3	34.12	1078	16.68	4.625	191.90	33, 38, 22
T4	32.97	1092	-59.00	-16.252	194.36	38, 21, 22
T1R	22.82	1055	23.00	6.446	187.83	
G15W: density, 816.9 kg/m^3; k, 0.1919[a] W/m•K						
T1	22.55	2461[b]	4.00	0.652	472.34	22, 23, 22
T2	23.78	2098[b]	23.42	4.135	402.57	22, 29, 22
T3	28.14	1425[b]	26.20	5.614	273.38	27, 33, 26
T4R	35.00	1296	38.30	7.369	248.65	33, 41, 26
T6	37.18	1274	-59.00	-13.370	244.41	41, 26, 26
G30W: density, 1000 kg/m^3; k, 0.2325[a] W/m•K						
T5A	22.42	4116[b]	26.20	2.712	957.01	22, 27, 22
T5B	28.55	5891[b]	32.80	2.838	1369.66	27, 34, 22
T5C	31.05	1534	-59.00	-10.003	356.66	34, 22, 22
T5D	23.33	6012[b]	26.20	2.244	1397.82	22, 27, 22
T5E	26.29	1942[b]	-26.20	-3.947	451.40	27, 22, 22
T6	27.82	1528	26.20	4.451	355.29	26, 32, 26
T7	33.30	1520	32.80	5.586	353.50	32, 38, 26
T8	35.43	1526	-59.00	-10.030	354.77	38, 26, 26

[a]k-value of gypsum-liquid wax.
[b]See text.

spanned the first 1.8 kiloseconds of each transient.The specific heat (C) was calculated from the experimental $k\rho C$ value using measured values of k and ρ.

The five C values for GOW increase with temperature and are described to 1% by

$$C\ (\mathrm{J/kg{\bullet}K}) = 159.5 + 3.0070\ \mathrm{T\ (K)}; \tag{32}$$

these are about 2% below values given by Eq. (14).

Three of the five C values for G15W are very large and indicate that a phase change was occurring during the transient. The other two C values average 1285 J/kg•K, which is 2% above the value in Table 8. Four of the eight values for G30W are large and are indicative of a phase change. The other four C values average 1527 J/kg•K, which is 4% above the value in Table 8. These four C values apply for gypsum containing liquid wax between 28 and 38°C (Fig. 15). The large apparent specific heat values were derived using the short-time solution

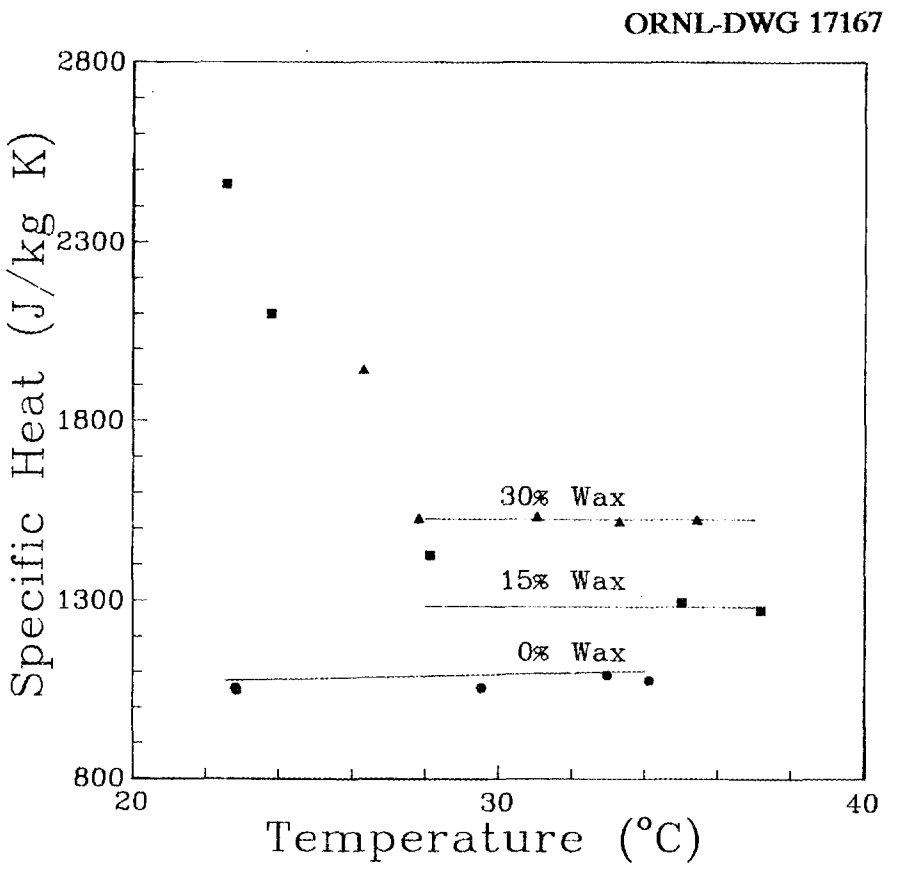

Fig. 15. Specific heat as a function of temperature for gypsum-wax specimen.

given in Eq. (4). This equation is for determining the specific heat only and does not apply for cases where a phase change is occurring. An analysis that includes the latent heat of the phase change is needed to treat these cases.

The experimental C values at 30°C for gypsum and the two composites fit the rule of mixtures:

$$C \text{ (composite, J/kg•K)} = 1070\,(1 - X_w) + 2589\,(X_w) \quad , \tag{33}$$

where X_w is the weight fraction of wax in the composite. This equation predicts a C (wax, 30°C) of 2589 J/kg•K, which is 9.5% higher than the corresponding states model.[20]

Figure 16 compares the temperature response for tests on gypsum with 0 wt % wax (T1R) and gypsum with 30 wt % wax (T5A). This figure shows that steady-state condition was reached in 20 ks for the GOW specimen but was not reached in over 60 ks for the G30W specimen. The latter data yielded a high C value, which is indicative of the wax phase change occurring during the test.

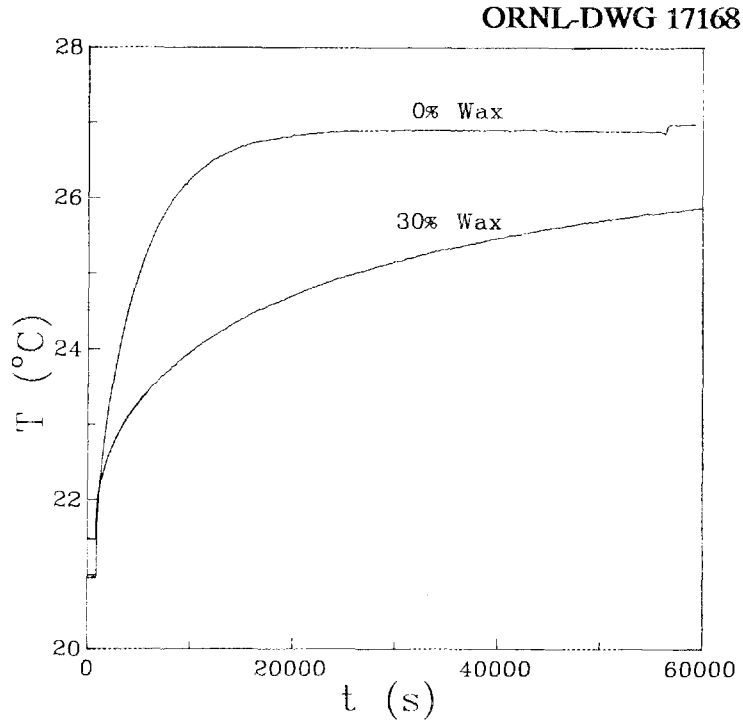

Fig. 16. Temperature vs time for gypsum without wax (GOW) and gypsum with 30 wt % wax (G30W).

Table 20 contains α values from 20 to 50°C that were calculated from the experimental values of ρ, k, and C for the three specimens. The α values for the gypsum without wax decrease with increasing temperature because of the increase of C with temperature. The α values for the composites decrease with increasing wax content, and the α (solid wax) values are 3 to 5% larger than the α (liquid wax) values. The experimental α values (Table 20) are 15 to 25% larger than the α values estimated from the literature (Table 8). The gypsum products have the lowest thermal mass ratios of the materials tested, less than 0.008 (Table 18). Thus close agreement should be achieved between the results of Methods 1 and 3.

The specific heat values from Method 3 for the gypsum without wax are an average 4.6%, or 49 J/kg•K, higher than those determined by Method 1. The values for gypsum with 15 or 30% liquid wax are in better agreement and average 1.0% (or 13 J/kg•K) high for G15W, and 1.0% (or 16 J/kg•K) low for G30W. At the lowest value of TMR, 0.004 for G30W, a difference of about 1% occurs in the values obtained from the two methods of analysis. We are unable to resolve which method yields the correct C value. The 4.6% difference for G0W may be associated with uncertainties in the starting time of the test. The ±1% agreement for G15W and G30W are within the limits of error of Eq. (5) for the data from Method 1.1. We believe the ±1% agreement is more representative than the 4.6% value. Because the experimental uncertainty in the k-values is about 1% and those in the C values are about 1%, this analysis yields a combined error in the α values of about 2%.

Table 20. Calculated thermal diffusivity for three gypsum-wax composites

	G0W	G15W	G30W
Percent wax	0	14.1	30
Density, kg/m^3	695.1	816.9	1000.0
C, J/kg•K	a	1285	1527
k, W/m•K	0.1780	0.1919[b]	0.2325[b]
	α, m^2/s x 10^7		
t, °C 20	2.460	(1.919)[c]	(1.565)
25	2.425	1.919	1.565
30	2.391	1.828	1.523
50	2.264	(1.828)	(1.523)

[a]Eq. (20).
[b]k of liquid-wax gypsum composite.
[c]Extrapolated.

6.2.2 Calcium Silicate Boards

Table 21 lists the results obtained by analyzing the 14 transient tests for the CS-1, CS-2, and CS-3 specimens using Eqs. (4) and (5), Method 2. Each specimen was subjected to positive and negative step changes in heat flux. The slope term in Eq. (5) was determined using the data that spanned the range 200 to 1800 s of each transient. The heat flux correction for the screen thermal mass was less than 2% for all 14 cases. The specific heat (C) was calculated from the experimental $k\rho C$ value using the measured values of ρ and the k-values calculated from the equations given in Table 21.

The 14 values of C for the calcium silicate test specimens are plotted in Fig. 17 and increase with temperature. Each of the transient tests with negative step changes in heat flux yielded low C values. If these are excluded, the remaining 11 values are described with an average deviation of 1.0% by

$$C = 951.5 + 2.556\ t\ . \tag{34}$$

Equation (34) yields a C^{24} of 1012.6 J/kg•K, which is 1.3% above the estimated value for C given in Table 10.

Table 22 contains thermal diffusivity (α) values calculated from the experimental values of ρ and C and the k-values calculated from the equations in Table 21. If the analyzed results from the cool-down transients are excluded, the following equations describe the α of the three specimens with an average percent deviation of less than ±0.4%:

$$\alpha\ (\text{CS-1})\ 10^7 = 2.221 - 3.81 \times 10^{-3}\ t\ , \tag{35}$$

$$\alpha\ (\text{CS-2})\ 10^7 = 1.679 - 1.65 \times 10^{-3}\ t\ , \text{ and} \tag{36}$$

$$\alpha\ (\text{CS-3})\ 10^7 = 1.483 - 2.12 \times 10^{-3}\ t\ , \tag{37}$$

Table 22 contains α values for the three calcium silicate test specimens calculated from these equations. The α values decrease with temperature and with increasing density. The α values are 19 to 28% lower than the estimated α values given in Table 10. The least dense samples, CS-1, yielded an average of 5.3% or 54 J/kg•K higher specific heat from Method 3 than from Method 2. Specific heat values from Method 3 for the medium density CS-2 are near those for Method 2, and yielded an average difference of 1.4% or 15 J/kg•K. The highest density calcium silicate had a slightly smaller difference of 1.3% or 14 J/kg•K. As in the case of C (GOW), we do not know which method is yielding the correct C (CS-1). The C values from Method 2 were used to obtain the α values given above.

Table 21. Summary of the thermophysical properties of calcium silicate derived from analysis of transient tests by Method 2

Transient test	Average temperature (°C)	k (Eq.) (W/m•K)	$k \bullet \rho$ (W•kg/m^{4}K)	$k \bullet \rho \bullet C$ (W^2•s/m^4•K^4)	C (J/kg•K)	α (m^2/s•10^7)
CS-1: density, 307.4 kg/m^3; k (Eq.) = 0.063842 + 6.3008 x 10^{-5} t						
1	25.65	0.06546	20.12	20177.8	1002.9	2.1236
2	28.14	0.06562	20.17	20259.9	1004.7	2.1250
3	32.76	0.06591	20.26	20776.6	1025.7	2.0907
4	40.48	0.06639	20.41	21435.3	1050.4	2.0537
5	50.15	0.06700	20.59	22014.3	1069.0	2.0392
6[a]	45.77	0.06673	20.51	20934.8	1020.8	2.1268
CS-2: density, 443.95 kg/m^3; k (Eq.) = 0.07264 + 7.98935 x 10^{-5} t						
1	26.40	0.07475	33.185	34081.2	1027.0	1.6395
2	34.67	0.07541	33.478	35210.7	1051.7	1.6151
3	49.38	0.07658	34.000	36661.0	1078.3	1.5997
4[a]	47.27	0.07642	33.927	34206.8	1008.3	1.7072
CS-3: density, 605.1 kg/m^3; k (Eq.) = 0.087021 + 7.9729 x 10^{-5} t						
1	26.22	0.08911	53.920	55462.3	1028.6	1.4317
2	37.20	0.08963	54.235	57055.9	1052.0	1.4080
3	44.10	0.09054	54.784	58884.2	1074.8	1.3921
4[a]	42.76	0.09043	54.719	54709.0	999.8	1.4948

[a]Cool-down transient.

ORNL-DWG BMG90-8

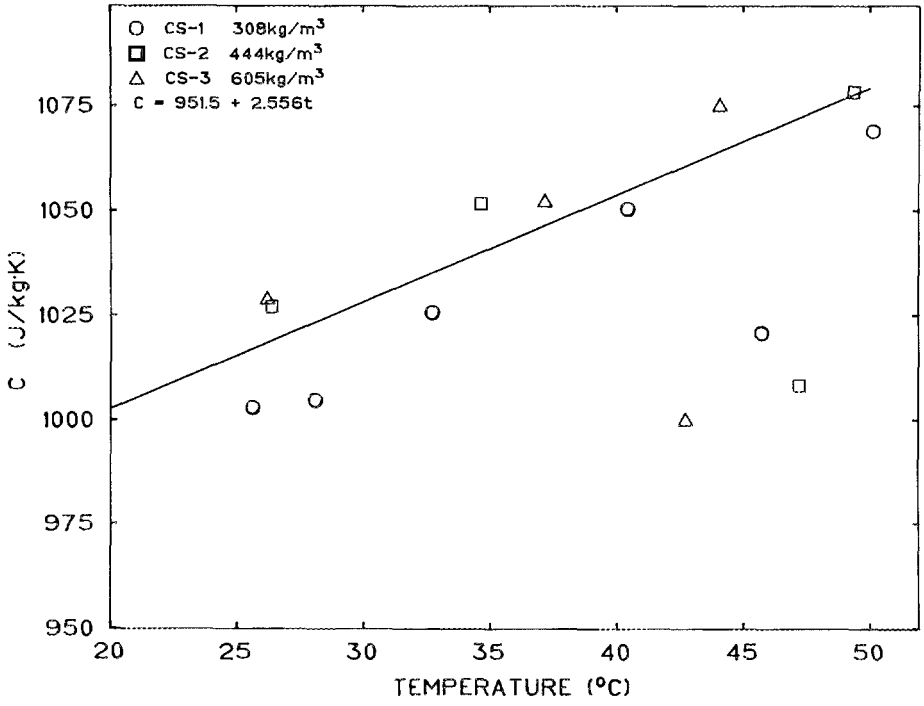

Fig. 17. Specific heat as a function of temperature for three calcium silicate insulations.

Table 22. Calculated thermal diffusivity for three calcium silicate specimens ($\alpha \times 10^7$, m^2/s)

		CS-1	CS-2	CS-3
Density, kg/m^3		307.4	443.95	605.1
t, °C	20	2.145	1.712	1.441
	24	2.130	1.639	1.432
	30	2.107	1.629	1.419
	50	2.031	1.596	1.377

6.2.3 Wood Products

Table 23 contains the results obtained by analyzing the 12 transient tests conducted on the wood products using Eqs. (4) and (5), Method 2. Each specimen was subjected to three positive and one negative step-change in heat flux. The slope term in Eq. (5) was determined using data that spanned the range 200 to 1800 s for each transient. The heat flux correction for the screen thermal mass was -1.03% for the WSF specimens, -1.09% for the DFP specimens, and - 0.85% for the SYPF specimens. The specific heat (C) was calculated from

Table 23. Summary of the thermophysical properties of wood products derived from analysis of transient tests by Method 2

Transient test	Average temperature (°C)	k(Eq.) (W/m•K)	k•ρ (W•kg/m^{4}K)	$k\rho$•C experimental (W^2 s/m^{4}K^2)	C (J/kg•K)	α (m^2/s x 10^7)
WSF: density, 451.5 kg/m^3; k (Eq.) = 0.09920 + 1.5537 x 10^{-4} t						
1	23.15	0.1028	46.465	76961.9	1656.3	1.3731
2	27.46	0.1035	46.77	78010.6	1668	1.3727
3	37.16	0.1050	47.45	81193.3	1711.7	1.3576
4[a]	42.15	0.1057	47.80	82344.4	1722.7	1.3575
DFP: density, 500.9 kg/m^3; k (Eq.) = 0.09786 + 1.6039 x 10^{-4} t						
1	23.14	0.1016	50.89	71235.0	1399.8	1.4490
2	30.39	0.1027	51.46	72593.3	1410.7	1.4534
3	43.66	0.1049	52.52	74642.0	1421.1	1.4737
4[a]	39.32	0.1042	52.175	73655.0	1411.7	1.4735
SYPF: density, 575.2/m^3; k (Eq.) = 0.1234 + 1.6153 x 10^{-4} t						
1	22.99	0.1271	73.34	115571.9	1575.9	1.3978
2	26.49	0.1277	73.66	120979.8	1642.3	1.3476
3	34.29	0.1289	74.39	124646.9	1675.5	1.3336
4[a]	38.46	0.1296	74.78	124818.6	1669.1	1.3457

[a]Cool-down transient.

the experimental values of $k\rho C$ using the measured values of ρ and the k-values calculated from the equations in Table 23.

The C values for each wood specimen (plotted in Fig. 18) span the range of 1400 J/kg•K to 1725 J/kg•K. Each wood product shows a different temperature dependence for C (i.e., C

ORNL-DWG BMG90-9

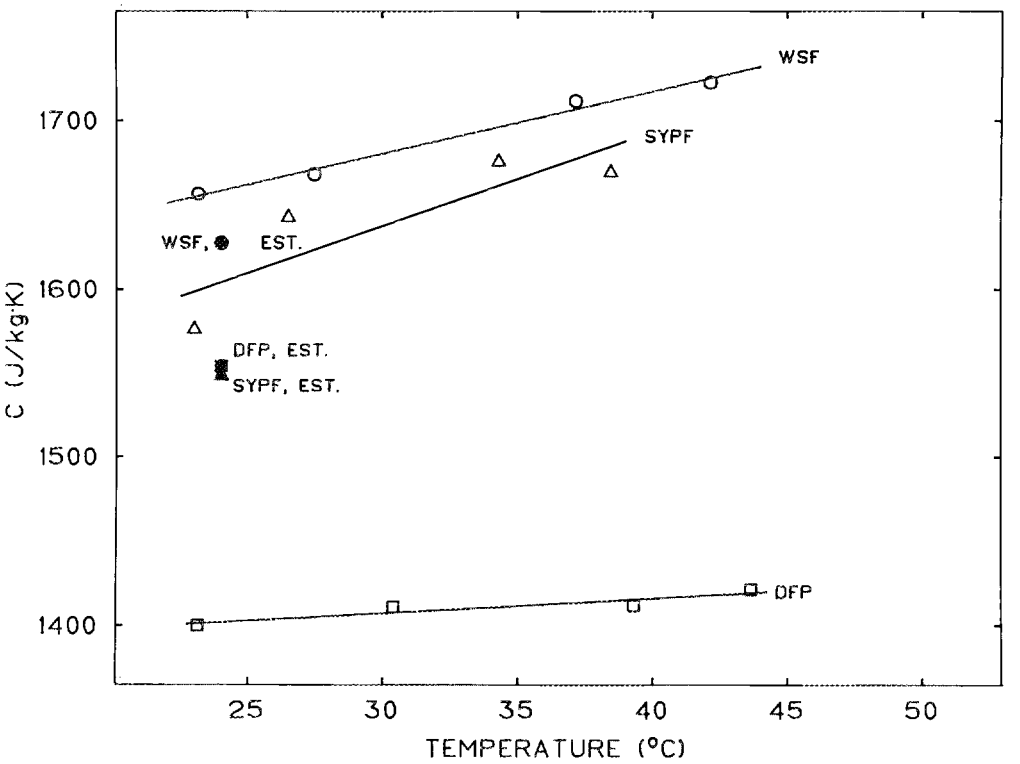

Fig. 18. Specific heat as a function of temperature for three wood products.

increases from DFP to SYP to WSF). The following equations describe the C results for these specimens:

$$C\ (\mathrm{WSF}) = 1569.7 + 3.6910\ t,\ \pm 0.16\%\ , \tag{38}$$

$$C\ (\mathrm{SYPF}) = 1470.2 + 5.5805\ t,\ \pm 1.2\%\ ,\ \text{and} \tag{39}$$

$$C\ (\mathrm{DFP}) = 1380.5 + 0.8874\ t,\ \pm 0.18\%\ . \tag{40}$$

For the WSF specimen, Eq. (38) yields a C (24) of 1658 J/kg•K; this is 1.9% above the estimated C given in Table 11. The SYPF has a lower moisture content than the WSF

specimen and has a lower C value. For SYPF, Eq. (27) yields a C^{24} of 1604 J/kg•K; this is 3.6% above the estimated C given in Table 12. The DFP specimen showed the lowest C values, and Eq. (40) yields a C^{24} of 1402 J/kg•K; this is 9.8% lower than the estimated C given in Table 12.

Table 23 contains thermal diffusivity (α) values calculated from the experimental values of ρ and C and the k-values calculated from the equations in Table 23. The following equations describe the α of the three specimens with an average percent deviation of less than ±1.2%:

$$\alpha\ (\text{WSF}) \times 10^{7} = 1.3968 - 9.7243 \times 10^{-4}\ t,\ \pm 0.16\%\ , \tag{41}$$

$$\alpha\ (\text{SYPF}) \times 10^{7} = 1.4471 - 2.9772 \times 10^{-3}\ t,\ \pm 1.18\%\ ,\ \text{and} \tag{42}$$

$$\alpha\ (\text{DFP}) \times 10^{-7} = 1.4156 + 1.3710 \times 10^{-3}\ t,\ \pm 0.18\%\ . \tag{43}$$

Table 24 contains α values for the three wood product test specimens calculated from these equations. The α values for the WSF and SYPF are about 20% lower than the estimated α values given in Table 12 and the DFP is 2% lower than the estimated α in Table 12.

Table 24. Calculated thermal diffusivity for three wood product specimens ($\alpha \times 10^{7}$, m^2/s)

		WSF	SYPF	DFP
Density, kg/m^3		451.5	575.2	500.9
t, °C	20	1.3773	1.3876	1.4430
	24	1.3735	1.3756	1.4485
	30	1.3676	1.3578	1.4567
	50	1.3482	1.2982	1.4841

The comparison of the Method 3 and Method 2 derived C values shows differences that increase with TMR. WSF had the smallest difference in the group, 21 J/kg•K or 1.3%. A 5.4% or 77 J/kg•K difference was found for DFP. The calculated values from Method 3 were 56 J/kg•K low for SYPF. Method 2 values of C were used to calculate α.

6.2.4 Plastic Cellular Foams

Table 25 contains the results obtained by analyzing three transient tests conducted on the polyisocyanurate (CFC-11) test specimen and 12 transient tests conducted on the extruded polystyrene (HCFC-142b) test specimen. This analysis used Eqs. (4) and (5), Method 2. Each specimen was subjected to positive and negative step changes in heat flux. The heat flux corrections for the heater thermal mass were large (Table 25). The slope term in Eq. (5) was determined using data that spanned the range of 200 to 1800 s for the polyisocyanurate specimen and 100 to 900 s for the extruded polystyrene specimen. The polystyrene specimen was tested three times after manufacture.

The C values obtained from each test of the cellular plastic foams is plotted in Fig. 19 and span the range of 1140 J/kg•K to 1680 J/kg•K. The C values for the polyisocyanurate specimens are highest; these are described with an average percent deviation of 0.21% by

$$C = 12681.1 + 9.4857\ t\ . \tag{44}$$

Equation (44) yields a C^{24} of 1496 J/kg•K; this is 1.9% above the estimated C given in Table 13. The C values for the extruded polystyrene specimen decrease as aging time increases. Equations to describe the C values are:

$$C\ (42\ \mathrm{d}) = 1103.6 + 6.084\ t,\ \pm 1.9\%\ , \tag{45}$$

$$C\ (131\ \mathrm{d}) = 1067.6 + 4.0294\ t,\ \pm 1.2\%\ ,\ \text{and} \tag{46}$$

$$C\ (227\ \mathrm{d}) = 1046.0 + 4.2128\ t,\ \pm 0.8\%\ . \tag{47}$$

Equation 47 yields a C^{24} of 1147 J/kg•K; this is 0.25% less than the estimate of C given in Table 13. Note that C (45 d) is greater than C (227 d); this effect may be due to inward diffusion of air and outward diffusion of HCFC-142b - a higher C being associated with the blowing agent. The value given in Table 13 coincides with calculated values for air and polystyrene.

Table 25 contains thermal diffusivity (α) values calculated from the experimental ρ and C values and the k-values calculated from the equations in Table 25. The following equations describe the α of these specimens with an average percent deviation of less than ±2%:

$$\alpha\ (\mathrm{PIR}) \times 10^{7} = 4.623 - 5.344 \times 10^{-3}\ t,\ \pm 0.20\%\ , \tag{48}$$

Table 25. Summary of the thermophysical properties of cellular plastic foams from analysis of transient tests by Method 2

Transient test	Average temperature (°C)	k(Eq.) (W/m•K)	k•ρ (W•kg/m^{4}K)	k•ρ•C experimental (W^2 s/m^4•K^2)	C (J/kg•K)	α (m^2/s x 10^7)	F applied (W/m^2)	F corrected (W/m^2)
PIR (CFC-11): density, 30.2 kg/m^3; k(Eq.) = 0.017941 + 9.90541 x 10^{-5} t								
1	27.25	0.02064	0.6223	951.868	1529.6	4.475	6.604	6.036
2	39.78	0.02188	0.6597	1082.21	1640.4	4.424	-41.271	-37.924
3	43.08	0.02221	0.6695	1125.39	1680.8	4.383	34.638	31.883
PS (HCFC-142b) 45 days: density, 30 kg/m^3; k(Eq.) = 0.02368 + 1.2618 x 10^{-4} t								
1	26.12	0.0260	0.7790	975.416	1250.2	6.941	6.604	5.833
2	33.52	0.0269	0.8059	1055.25	1309.4	6.857	11.915	10.573
3	46.82	0.02846	0.8527	1228.56	1440.8	6.593	22.758	20.361
4	52.37	0.0291	0.8718	1203.59	1380.5	7.036	-41.273	-36.881
PS (HCFC-142b) 131 days: density, 30 kg/m^3; k(Eq.) = 0.02567 + 1.1831 x 10^{-4} t								
1	25.98	0.02874	0.8610	996.32	1157.1	8.290	6.605	5.841
2	33.00	0.0296	0.8861	1086.41	1226.1	8.058	11.915	10.589
3	46.03	0.0311	0.9325	1155.42	1239.0	8.378	25.350	23.500
4	52.52	0.0319	0.9557	1226.35	1283.2	8.233	-44.862	-40.470
PS (HCFC-142b) 227 days: density, 30 kg/m^3; k(Eq.) = 0.02602 + 1.2181 x 10^{-4} t								
1	26.04	0.0292	0.8746	1021.80	1168.3	8.342	6.606	5.851
2	32.78	0.0300	0.8992	1047.75	1165.2	8.594	11.883	10.528
3	45.78	0.0310	0.9466	1178.52	1244.9	8.312	26.383	23.555
4	52.23	0.03238	0.9702	1228.61	1266.4	8.534	-44.866	-40.138

ORNL-DWG BMG90-10

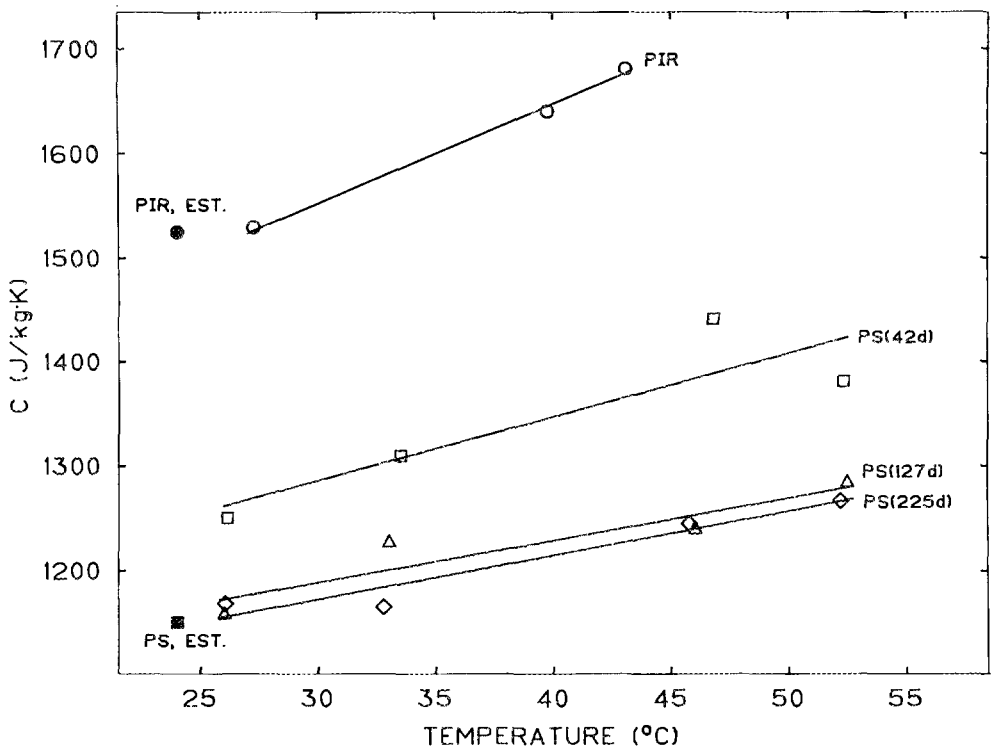

Fig. 19. Specific heat as a function of temperature for cellular plastic foams.

$$\alpha \text{ (PS [45 d])} \times 10^7 = 6.926 - 1.7344 \times 10^{-3}\, t, \pm 1.92\% , \quad (49)$$

$$\alpha \text{ (PS [131 d])} \times 10^7 = 8.121 + 3.012 \times 10^{-3}\, t, \pm 1.27\% , \text{ and} \quad (50)$$

$$\alpha \text{ (PS [227 d])} \times 10^7 = 8.383 + 1.599 \times 10^{-3}\, t, \pm 1.34\% . \quad (51)$$

Table 26 contains α values for these cellular plastic foams calculated from these equations.

Table 26. Calculated thermal diffusivity for cellular plastic foams
($\alpha \times 10^7$, m^2/s)

		PIR (CFC-11)	PS (HCFC-142b)		
Density, kg/m^3		30.2	30.0	30.0	30.0
Age, d		398	45	131	227
t, °C	20	4.516	6.891	8.181	8.415
	24	4.495	6.888	8.170	8.421
	30	4.463	6.875	8.206	8.447
	50	4.356	6.833	8.311	8.529

The α values for PIR (CFC-11) are between the values estimated in Table 13. The α values for the PS (HCFC-142b) started out greater than the initial α estimated in Table 13 and exceed the α (beyond 100 d) value by 2.7%.

Because of the high TMR's for these materials, Method 2 was used to find their specific heats. Method 2 has no fundamental basis, and large differences between the calculations resulted: PIR-CFC-11, -21% or -335 J/kg•K; PS @ 45 d, +7.7% or 103 J/kg•K; PS @ 131 d, +8.3% or 102 J/kg•K; and PS @ 227 d, +9.1% or 109 J/kg•K. The TMRs for these materials were approximately 0.14 for the PS and 0.24 for the PIR. If the *C* values for the plastic foams from Method 3 were used to compute the α values, then the α (PIR) would increase by about 25% and the α (PS) would decrease by about 10%. Table 27 summarizes the materials with the highest TMR studied.

Table 27. Summary of differences between calculation methods

Material	TMR	Methods	Delta C[a]	% Difference
GOW	0.0075	3 and 1	49	4.6
G15W	0.0055[b]	3 and 1	13[b]	1.0[b]
G30W	0.0038[b]	3 and 1	-16[b]	-1.0[b]
CS-I	0.0231	3 and 1	54	5.3
CS-II	0.0164	3 and 1	15	1.4
CS-III	0.0121	3 and 1	14	1.3
WSF	0.0077	3 and 1	21	1.3
DFP	0.0105	3 and 1	77	5.4
SYP	0.0065	3 and 1	-56	-3.4
PIR-CFC	0.237	3 and 2	-335	-20.7
PS @ 45	0.132	3 and 2	103	7.7
PS @ 130	0.144	3 and 2	102	8.3
PS @ 230	0.145	3 and 2	109	9.1

[a]C for M3 minus *C* for M1 or M2.
[b]Gypsum plus liquid wax only.

7. DISCUSSION OF RESULTS

Discussed are potential improvements in the measurement equipment suggested by the analyses of the transient tests and a comparison of the test results obtained on these building materials.

7.1 MEASURING EQUIPMENT AND ANALYSIS DEVELOPMENT

The existing UTHA equipment and procedure for use in a two-sided or one-sided steady-state mode of operation provides *k*-values with an uncertainty of less than 2% for homogeneous building materials of the type described in this report. Thus the UTHA has achieved a satisfactory state of development that compares favorably with other absolute, longitudinal heat flow techniques such as guarded hot plates. The UTHA is a mechanically, electrically, and thermally simple apparatus that provides good sampling on large area specimens. It has been used on a wide variety of building insulations and building materials. The measurement errors are positive above room temperature, and the tester is readily modeled. It is a valuable technique for use by the building materials research community.

In contrast, the existing UTHA equipment and procedure for the transient mode of operation with positive and negative step-changes in heat flux is relatively new and requires further research to reach a mature stage of development. For the building materials included in this report, satisfactory results were obtained on specimens that had low values for the ratio of the thermal mass of the heater to that of the specimen (TMR). The existing heater thermal mass, 0.5 $t_{sc}\ \rho\ C$, is about 300 J/m^3•K/m^2. Table 28 lists the thermal mass values and TMR for some of the tested materials. For the materials with TMR values below 0.025, the

Table 28. Specimen thermal mass and the thermal mass ratio (300 J/m^3•K)

Specimen	Thermal mass $L\rho C$ (J/m^{3}K)	Thermal mass ratio (TMR)
GOW, gypsum	36630	0.008
CS-1, 307 kg/m	11854	0.025
WSF	36728	0.008
PS (PS, double thickness, SS)	1755 (3510	0.170 (0.020)
PIR (PIR, double thickness, SS)	1435 (2870)	0.209 (0.025)

heat flux correction for the heater thermal mass was 1% or less. However, for the cellular plastic foams the heat flux correction by Method 2 was 9 to 13%; this corresponds to a 21 to 30% correction in the value for $k\rho C$, since the heat flux term is squared. These large corrections increase the measurement uncertainty for these materials, and this effect decreases the applicability and value of the technique. To reduce this technique limitation, several alternate paths are being pursued.

An alternate heater with a lower thermal mass would decrease the TMR and reduce the heat flux correction. For example, we have obtained a type 316 stainless steel wire screen that has a thickness of 117 x 10^{-6} m (0.0046 in.), ρ of 2350 kg/m^3, and C (estimated) of 525 J/m^3•K. Thus a type 316 stainless steel heater of this thickness would have a thermal mass that is about 70 J/m^3•K; this is 25% of the existing Nichrome heater. This type 316 stainless steel heater would decrease the TMR values given in Table 28 by a factor of 4 and reduce the needed corrections to the heat flux change and the $k\rho C$ product. Table 28 shows that doubling the specimen thickness and using a stainless steel heater would yield TMR values below 0.03. We should test this concept and seek alternative systems that yield an improvement by a factor of 10 or more over the existing Nichrome screen wire heater. System requirements include (1) a low thermal conductivity, such as metal alloy (Nichrome or stainless), or a heavily doped semiconductor; (2) a low thickness, such as a screen produced from small diameter wires [the screen thickness is about 2.6 times the wire diameter, so wires with a diameter of 25 by 10^{-6} m (0.001 in.) would improve the thermal mass by a factor of 10]; and (3) mechanical ruggedness to allow instrumentation and specimen changing without damage. A vapor-deposited metal film on a thin plastic membrane might obtain the desired low thermal mass. We are currently exploring each of these options. Further work on models of the transient system could provide improved procedures to analyze the thermal response of the specimen heater–specimen composite. Both existing means to correct the measured results, Method 2 and Method 3, derive from this type of approach.

The heater is a screen in the experiment. This configuration may effect the response of the material at x equal zero, as heat must "spread out" from the heater. This effect has not been included in the current model. A major gap exists in that there are no SRMs for transient tests, so confirmation of a testing procedure is difficult. Materials with known specific heat are required to establish which analysis method is correct. This report has not included a discussion of transient tests and analyses that were conducted during the early

stages of development of the UTHA on SRM 1450b, SRM 1451, and a low-density fiberglass blanket.[3, 4, 37, 38] The TMR values for these materials were in the range of 0.05 (SRM 1450b) to 0.5 (SRM 1451). Clearly these TMR values are in the region that requires a significant correction. The treatments of these results raised another important aspect of the transient behavior of such low-density insulations -- the role of radiative heat transport. All of the current analyses presume that the heat transport is by a diffusive-conduction process that occurs at the speed of sound. We do not believe that this is the case for radiative heat transport, which may be diffusive but occurs at the speed of light. We need to reexamine modeling analyses to show the impact of (1) thermal mass of the transient system components for diffusive-conduction heat transport and (2) diffusive-radiative heat transport on the presumed diffusive-conductive heat transfer. In addition, we should extend our literature search for thermophysical properties, particularly measurements of the heat capacity of building materials. Our previous search on SRMs and fiberglass blankets led to measurements of specific heat of these materials by a differential scanning calorimeter[39]. The specific heat of moist specimens was significantly larger than the specific heat of dry specimens because of the effect of latent heat of vaporization and desorption of moisture. The presence of a phenolic binder on the specimens precluded testing of dry specimens (i.e., all specimens containing a phenolic binder absorb moisture rapidly). This phenomena impacts any transient test conducted in an ambient environment containing moisture. A compilation of available thermophysical properties may help in the identification of specimens for transient tests and in the development of transient analysis procedures. In general, the literature is limited on the specific heat of insulating and building materials. This limitation could lead to the need for obtaining a technique to measure this property, and such items are commercially available.

7.2 THERMOPHYSICAL PROPERTIES OF BUILDING MATERIALS

Sections 5 and 6 provide descriptions of the test specimens and present steady-state and transient test results on the individual test specimens. The test results are compared with estimated properties and are used to calculate the specimen thermal diffusivity. This subsection compares the thermophysical properties for the four sets of building materials.

Figure 20 shows the k of the four sets of building materials from 20 to 50°C. The range of k-values is from 0.02 to 0.24 W/m•K. The high-density gypsum specimens have the highest k-values of the tested materials, and the wax-containing materials have a higher k when the

ORNL-DWG BMG90-11

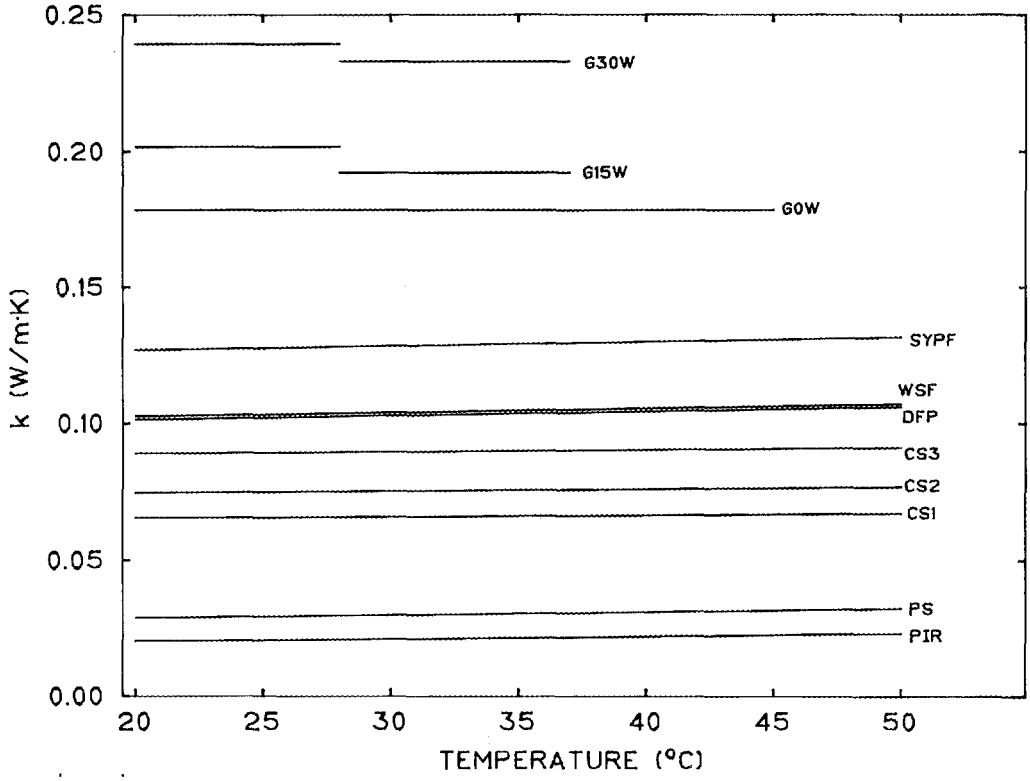

Fig. 20. Thermal conductivity as a function of temperature for four sets of materials.

wax is solid than when the wax is liquid. The k of gypsum without wax is a constant, 0.178 W/m•K; this is 17% greater than the value given by the American Society of Heating, Refregerating, and Air Conditioning Engineers.[15] The k-values for the wood products are in the range of 0.10 to 0.13 W/m•K and increase slowly with temperature. The southern yellow pine k-value is near 0.12 W/m•K, and the WSF and DFP have nearly equal k-values, 0.10 W/m•K. The calcium silicate insulation k-values are in the range of 0.065 to 0.09 W/m•K, building increase with density, and increase slowly with temperature. The cellular plastic foam test specimens show the lowest k-values, and these increase slowly with temperature. The PS specimen has a k near 0.030 W/m•K; the PIR specimen, a k near 0.020 W/m•K.

Figure 21 shows the specific heat of the four sets of building materials as a function of temperature from 20 to 50°C. The C values are in the range of 1000 to 1750 J/kg•K, and the order of C values differs from that of the k-values for these materials. All C values increase with temperature. The lowest C values were found for the three calcium silicate

ORNL-DWG BMG90-12

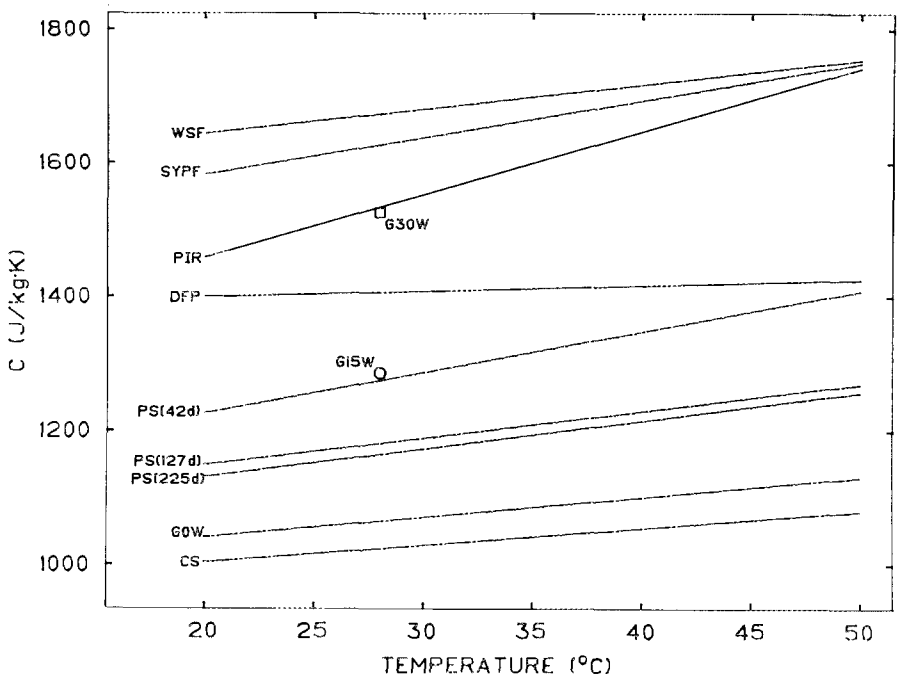

Fig. 21. Specific heat as a function of temperature for four sets of building materials.

specimens, and these did not depend on density. The highest *C* values were found for the moisture-containing wood products WSF and SYPF. The gypsum (without wax) *C* value was slightly greater than that of the CS specimens and increased dramatically with wax content (C[G30W] ~ 1.5 C [GOW]). The *C* value of the PS specimens decreased with age and were about 2/3 of the *C* value measured for the PIR (CFC-11) specimen. The *C* value of the DFP was near 1400 J/kg•K, and the WSF and SYPF were between 1600 and 1750 J/kg•K.

Figure 22 shows the thermal diffusivity, $k/\rho C$, for the four sets of building materials as a function of temperature from 20 to 50°F. The α values are in the range of 1.9 by 10^{-7} to 8.6 by 10^{-7} m^2/s. The wood products show the lowest α values; the plastic cellular foams, the highest. In general, all α values decrease slowly with temperature in this temperature range. All three wood products have α values near 1.4×10^{-7} m^2/s. The calcium silicate α values decrease with increasing density from near 2×10^{-7} to near 1.4×10^{-7} m^2/s. The gypsum (without wax) has a α near 3.4×10^{-7} m^2/s, and the wax additions lower this to 1.9×10^{-7} m^2/s (G15W) and 1.5×10^{-7} m^2/s (G30W). The PIR (CFC-11) α value is near 4.5×10^{-7} m^2/s, and the PS α values increase with age from near 6.9×10^{-7} m^2/s to near 8.5×10^{-7} m^2/s. As noted

ORNL-DWG BMG90-13A

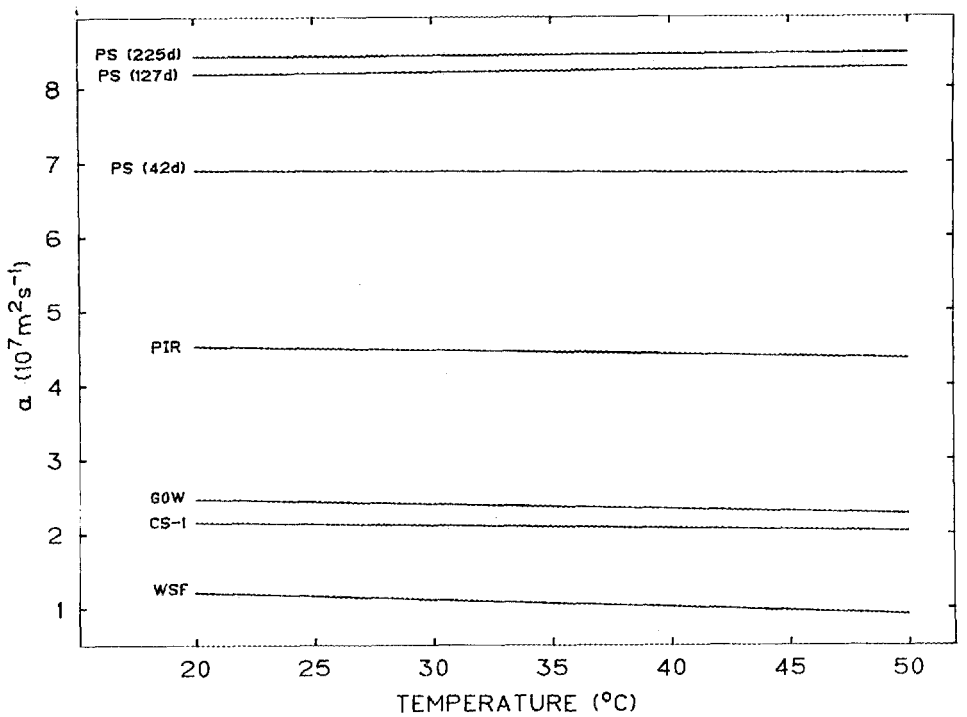

ORNL-DWG BMG90-13B

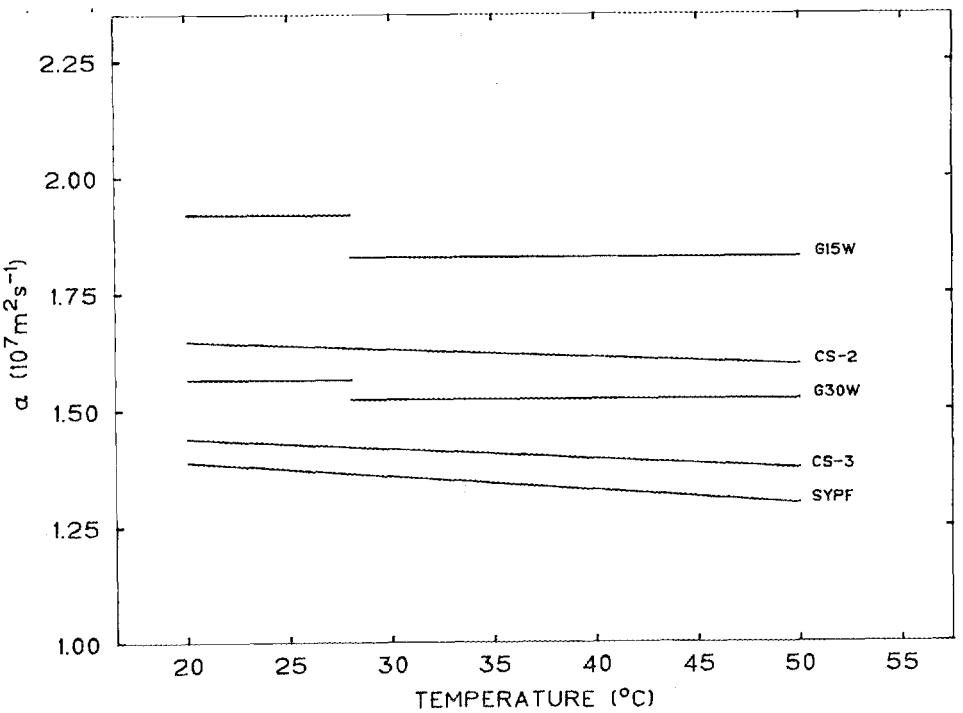

Fig. 22. Thermal diffusivity of four sets of building materials as a function of temperature from 20 to 50° C.

earlier, the α values for the dense building materials were only within ±30% of the estimated values, but the α values for the cellular plastics were within ±5% of the estimated values.

Finally, Table 29 contains values of the thermal response parameter, $k\rho C$, and the values of $(k\rho C)^{-1/2}$ for the individual test specimens at 24°C. Both parameters are a direct result of the analysis of the transient tests and are interesting material thermophysical properties. The $k\rho C$ values for these materials show a range of values from 900 to over 350,000 $W^2 \cdot s/m^4 \cdot K$, or a factor of 400. The $(k\rho C)^{-1/2}$ values show a range from 1.7×10^{-3} to over 33×10^{-3}, or a factor of 20. As Eq. (4) shows, the latter parameter indicates the expected change in temperature as a function of $(\text{time})^{1/2}$ after the application of a step-change in heat flux. For the denser building materials the rate of change decreases with increasing density and with increasing wax content for the gypsum specimens. For the cellular plastic foams the rate of change is significantly greater than for the other building materials. The $(k\rho C)^{-1/2}$ values are lowest for the gypsum specimens containing wax, and none of our analyses to date include the effect of the heat of fusion of the wax.

8. CONCLUSIONS AND RECOMMENDATIONS

Although the primary purpose of this report is to describe the transient mode of operation of the UTHA, the conclusions and recommendations about steady-state results are also included.

8.1 CONCLUSIONS

1. Steady-state and transient modes of operation of the UTHA yielded thermophysical properties (k, C, and α) of four types of building materials (i.e., gypsum with and without wax, calcium silicate insulations, wood products, and cellular plastic foams) from 24 to 50°C.

2. Standard reference materials, SRM 1450b and SRM 1451, were retested in the UTHA in 1990 and agreed with NIST values to 1.1 and 0.3%, respectively; this confirmed the ±1.2% most probable uncertainty for UTHA k-values.

3. A procedure was developed to operate the UTHA in a transient mode by applying a step-change in heat flux to specimens that were initially isothermal or that had a steady imposed temperature gradient. The procedure used a computer to control the test and to record the temperature-time behavior of the thin heater.

Table 29. Thermal response parameters at 24°C for the building material test specimens

Code	Materials	Density (kg/m^3)	Specific heat ($J/kg \cdot K$)	Thermal conductivity ($W/m \cdot K$)	Thermal response factors: $k\rho C$ ($W^2 \cdot s/m^4 \cdot K^2$)	Thermal response factors: $(k\rho C)^{-1/2} \times 10^3$ $m^2 \cdot K/W \cdot s^{1/2}$
GOW	Gypsum board	695.1	1052.6	0.1765	129138	2.738
G15W	Gypsum board 14.1 wt % wax	816.9	1285	0.1919	201440	2.228
G30W	Gypsum board 30 wt % wax	1000	1527	0.2325	355027	1.678
CS1	Calcium silicate 1	307.4	1012.8	0.065	20276	7.023
CS2	Calcium silicate 2	443.9	1012.8	0.074	33276	5.482
CS3	Calcium silicate 3	605.1	1012.8	0.089	54534	4.282
WSF	White spruce flooring	451.5	1658.3	0.1023	76679	3.611
DSF	Douglas fir plywood	500.9	1401.8	0.1010	70791	3.758
SYPF	Southern yellow pine	575.2	1604.1	0.1266	117176	2.921
PS	Polystyrene	30.0				
	age: 25 d					
	45 d		1249.2	0.0267	1000.6	31.613
	74 d					
	127 d		1164.3	0.0285	995.5	31.695
	227 d		1147.1	0.0289	994.5	31.710
PIR	Polyisocyanurate (CFC-11)	30.2	1495.8	0.01992	898.4	33.364

4. Experimental values for the product $k\rho C$ were determined from the temperature change of the thin heater that is a linear function of the square root of time after the step-change in heat flux. The error in the product $k\rho C$ was less than 1% for building materials; $(k\rho C)^{-1/2}$ values were below 10 $m^2K/W\sqrt{s}$ (i.e., densities above 300 kg/m^3 and low values of TMR). However, for the cellular plastic foams with $(k\rho C)^{-1/2}$ values above 30 $m^2K/W\sqrt{s}$ (i.e., densities near 30 kg/m^3 and large TMR values), alternative analyses were required because of the large relative thermal mass of the heater, and larger differences were found for $k\rho C$.

5. For each of the materials tested, published data were used to estimate k, C, and α values. The test results for k, C, and α were compared with these estimated properties, and α differences of up to ±30% were noted for the denser materials. The differences noted for the α of the cellular plastic foams were less than ±3% and, thus, were in the expected range.

6. Each of the thermophysical properties of each type of building material was tabulated, described by equations, and discussed in detail. The specific heat and thermal diffusivity are valuable materials characterization properties. This emphasizes the value of obtaining data from the UTHA in the nonsteady-state condition that precedes steady state.

8.2 RECOMMENDATIONS

1. Alternate paths should be pursued to obtain and to test a thin heater with a thermal mass that is less than 10% of the existing Nichrome heater (300 $J/m^2 \bullet K$) and to increase the test specimen thickness. This could extend the applicability of the UTHA in the transient mode to building insulations with densities in the range 10 to 30 kg/m^3.

2. The analyses of the heat-up step-changes in heat flux were more consistent than those for the cool-down step-changes in heat flux. Additional tests and analyses should be made to see if smaller cool-down step-changes in heat flux improve the agreement.

3. Further development is needed of the techniques for analysis of the transient data to increase the confidence in the $k \bullet \rho \bullet C$ products on low-density building materials. These analyses should include the impact of both diffusive-conductive and diffusive-radiative heat transport phenomena on the thermal response of the heater and should reexamine transient results obtained on low-density fiberglass, SRM-1451, and SRM 1450b.

4. A literature search of the thermophysical properties (k, ρ, C, and α) of building materials should be initiated to identify existing data and data gaps. This would provide a basis for future tests and identify the value of obtaining means for direct measurement of C.

5. Additional specific research should be conducted on the specimens tested to date.

5.1. Gypsum containing wax. Additional specimens containing a wax from an alternate source exist and should be tested in a modified UTHA. The capacity of the cold plate cooling units only allows cold plate temperatures of about 20°C. Units to cool the plates to 0°C are needed to allow measurements at lower mean temperatures for all materials and particularly for tests of gypsum containing wax from a solid wax state. These tests would be complemented by predictions of gypsum-wax behavior through the solid-liquid phase change to estimate the enhanced thermal performance.

5.2. Calcium-silicate insulations. We should encourage the producers of high-temperature insulations to develop and to apply a version of the UTHA that would operate from 24 to 650°C. An alternative would be to prepare an unsolicited proposal for the work to be done at ORNL with their guidance and financial support.

5.3. Wood products. Transient and steady-state tests using the UTHA should proceed as rapidly as possible on the remaining eight specimens from the Forest Products Laboratory Materials Bank. This is particularly important because the existing predictive equations for k of wood products overestimate k by 10 to 20%.

5.4. Plastic Cellular Foams. The measured k, C, and α results for polystyrene show large changes with age. Specific tests should be initiated to confirm this for new specimens of polystyrene and polyisocyanurate with alternative blowing agents.

9. ACKNOWLEDGMENTS

The authors express their appreciation to those who supplied the test specimens described in this report. J. J. Tomlinson and R. J. Kedl, ORNL, supplied the gypsum containing wax specimens, funded our studies of these materials, and reviewed our manuscript on the thermophysical properties of their specimens. T. Whitaker, PABCO, supplied the calcium silicate test specimens. Susan L. LeVan, Forest Products Laboratory, supplied specimens from their materials bank. P. Hendrickson, Dow Chemical USA, supplied the extruded polystyrene specimens. The Steering Committee of the Cooperative Project provided the polyisocyanurate boardstock. We also thank T. F. Hutton for developing the HP computer program, F. J. Weaver for making the figures and conducting some of the tests, G. L. Burn and S. M. Wilson for preparing the manuscript. Finally, we thank K. E. Wilkes, J. E. Christian, and T. G. Kollie, ORNL, for their reviews.

10. REFERENCES

1. J. P. Moore, D. L. McElroy, and S. H. Jury, *A Technique for Measuring the Apparent Thermal Conductivity of Flat Insulations*, ORNL/TM-6494, Union Carbide Corporation Nuclear Division, Oak Ridge National Laboratory, October 1979.

2. J. P. Moore, D. L. McElroy, and S. H. Jury, *A Technique for Measuring the Apparent Thermal Conductivity of Flat Insulations*, Plenum Pr., New York, 1983, pp. 727–35, (J. G. Hust, ed., *Thermal Conductivity*, Vol. 17).

3. D. L. McElroy, R. S. Graves, D. W. Yarbrough, and T. W. Tong, *Nonsteady State Behavior of Thermal Insulations*, High-Temperatures - High Pressures 17, 1985, pp. 395–401.

4. D. L. McElroy, R. S. Graves, D. W. Yarbrough, and J. P. Moore, *A Flat Insulation Tester That Uses an Unguarded Nichrome Screen Wire Heater*, Guarded Hot Plate and Heat Flow Meter Methodology, ASTM STP 879, ed. C. J. Shirtliffe and R. P. Tye, American Society for Testing and Materials, Philadelphia, 1985, pp. 121–39.

5. R. S. Graves, D. W. Yarbrough, and D. L. McElroy, *Apparent Thermal Conductivity Measurements by an Unguarded Technique*, Thermal Conductivity, Vol. 18, ed. T. Ashworth and D. R. Smith, Plenum Press, New York, 1985, pp. 339-55.

6. *Standard Test Method for Steady-State Thermal Transmission Properties by Means of the Thin-Heater Apparatus*, ASTM C1114-89, 1989 Annual Book of Standards, Vol. 04.06, American Society for Testing and Materials, Philadelphia, 1989, pp. 600–606.

7. R. S. Graves, D. L. McElroy, D. W. Yarbrough, and H. A. Fine, *The Thermophysical Properties of Gypsum Boards Containing Wax, Thermal Conductivity*, Vol. 21 (in press), Plenum Press, Lexington, Ky, October 15-18, 1989.

8. T. F. Hutton, ORNL, developed the HP program for transient testing.

9. J. P. Moore, R. K. Williams, and R. S. Graves, *Precision Measurements of Thermal Conductivity, Electrical Resistivity and Seebeck Coefficients from 80 to 400 K and their Application to Pure Molybdenum*, Rev. Sci. Instruments 45, 87–95, (1974).

10. H. S. Carslaw and J. C. Jaeger, *Conduction of Heat in Solids*, Oxford Pr., Fair Lawn, N. J., (1976).

11. H. Domingos and D. Voelker, "Transient Temperature Rise in Layered Media", *J. of Heat Transfer* 98, 329–30 (1976).

12. The gypsum board stock was obtained from U.S. Gypsum, Chicago, Illinois.

13. R. J. Kedl, ORNL, produced the boards, and process details are available from him.

14. J. F. Malloy, *Thermal Insulation*, Van Nos. Reinhold, New York, 1969.

15. *ASHRAE Handbook*, "1985 Fundamentals," Chapt. 23, Atlanta, GA, 1985.

16. K. K. Kelley, J. C. Southard, and C. T. Anderson, *Thermodynamic Properties of Gypsum and its Dehydration Products*, Tech. Paper 625, Bureau of Mines, 1941, p. 73.

17. W. M. Latimer, J. F. G. Hicks, Jr., and P. W. Schultz, "The Heat Capacities and Entropies of Calcium and Barium Sulfates from 15 to 300 K, The Entropy and Free Energy of Sulfate Ion," J. Chem. Phys. 1, 620 (1933).

18. Y. S. Touloukian and E. H. Buyco, *Specific Heat, Nonmetallic Solids*, Vol. 5, Plenum Pr., New York, 1970.

19. D. W. Yarbrough and Chi-Ning Kuan, *The Thermal Conductivity of Solid N-Eicosane, N-Octadecane, N-Heptadecane, N-Pentadecane, and N-Tetradecane*, *Thermal Conductivity*, Vol. 17, ed. J. G. Hust, Plenum Pr., New York, 1982, pp. 265-74.

20. B. C. Sakiadis and J. Coates, "Prediction of Specific Heat of Organic Liquids," *AIChE J.* 2(1), (1956).

21. A. Eucken, *Ceram. Abstr. 11*(11), 576 (1932).

22. The calcium silicate insulation test specimens were supplied by T. Whitaker, PABCO, Fruita, CO.

23. *Physical Characteristics of PABCO Super Cal Temp Calcium Silicate Pipe and Block Insulation*, PABCO Insulation Division, Fruita, CO, Rev. 5/77.

24. *Standard Specification for Calcium Silicate Block and Pipe Thermal Insulation*, ASTM C 533-85, 1989 Annual Book of Standards, Vol. 04.06, American Society for Testing and Materials, Philadelphia, 1986, pp. 178-81.

25. *Standard Specification for Structural Insulating Board, Calcium Silicate*, C 656-79a, 1989 Annual Book of Standards, Vol. 04.06, American Society for Testing and Materials, Philadelphia, 1989, pp. 254-56.

26. S. H. Jury, D. L. McElroy, and J. P. Moore, *Pipe Insulation Testers*, Thermal Transmission Measurements of Insulation, ASTM STP 660, ed. R. P. Tye, American Society for Testing and Materials, Philadelphia, 1978, pp. 310-26.

27. N. E. Hager, Jr., *Recent Developments with the Thin-Heater Thermal Conductivity Apparatus*, Guarded Hot Plate and Heat Flow Meter Methodology, ASTM STP 879, ed. C. J. Shirtliffe and R. P. Tye, American Society for Testing and Materials, Philadelphia, 1985, pp. 180-90.

28. The wood flooring stock was supplied by Susan L. LeVan, Forest Products Laboratory Materials Bank, Madison, Wisconsin 53705-2398, from the Forest Products Laboratory Materials Bank.

29. A. TenWolde, J. D. McNatt, and L. Krahn, *Thermal Properties of Wood and Wood Products for Use in Building*, ORNL/Sub/87-21697, Martin Marietta Energy Systems, Oak Ridge National Laboratory, September 1988.

30. The polystyrene board stock was produced in the Dow plant in Joliet, IL on July 25, 1989. The material was supplied by P. Hendrickson, Dow Chemical USA, Granville, Ohio.

31. The polyisocyanurate boardstock was produced by the Atlas Roofing Corporation at their plant in East Moline, IL, on June 1, 1989.

32. W. R. Strzepek, "Cellular Insulations," Chapt. 3.4 in *Handbook of Applied Thermal Design*, McGraw, New York, 1988.

33. L. L. Sparks, *Low-Temperature Properties of Expanded Polyurethane and Polystyrene*, Thermal Insulation Performance, ASTM STP 718, ed. D. L. McElroy and R. P. Tye, American Society for Testing and Materials, Philadelphia, 1989, pp. 431-52.

34. A. V. Liukov et al., *A Study of Thermophysical Properties of Construction Materials in a Temperature Range from 10 to 400 K*, Heat Transmission Measurements in Thermal Insulations, ASTM STP 544, American Society for Testing and Materials, Philadelphia, 1974, pp. 290-96.

35. D. L. McElroy et al., "The Technical Viability of Alternative Blowing Agents in Polyisocyanurate Roof Insulation, Part 3, Acceleration of Thermal Resistance Aging Using Thin Boards," paper in *Proceedings of the Polyurethanes '90 Conference, Orlando, October 1-4, 1990.*

36. Leon R. Glicksman, Massachusetts Institute of Technology, personal communication to D. L. McElroy, ORNL, Feb. 26, 1990.

37. G. Llewellyn, ORNL, personal communication to D. L. McElroy, ORNL, 1984.

38. J. K. Wood, "Transient Heat Transfer in Fibrous Insulation," master of science thesis, Tennessee Technological University, Cookville, TN, 1985.

39. J. G. Hust, J. E. Callanan, and S. A. Sullivan, *Specific Heat of Insulations, Thermal Conductivity*, Vol. 19, Plenum Press, New York, 1988, pp. 533–50.

APPENDIX A

FINITE DIFFERENCE MODEL EMPLOYED IN THE DEVELOPMENT OF METHOD 3

As mentioned in Sect. 4.3, a finite difference model was employed to generate the data used to develop Method 3 for the analysis of the transient test results. The development of this model follows.

The heat transfer problem is for transient unidirectional heat flow by conduction in an infinite slab of thickness L and a thin heater of thickness 0.5 t_{sc}. The boundary of the slab at x equal L is maintained at constant temperature $T(0)$. The boundary at x equals zero is in intimate contact with the thin heater. The heater has a finite thermal mass, 0.5 $t_{sc} \bullet \rho_{sc} \bullet C_{sc}$, and high thermal conductivity relative to the slab. The slab may initially be isothermal or have a linear temperature gradient. The desired results are the temperature of the heater as a function of time after a step-change in the power is applied to the heater.

The implicit finite difference method was used to solve the above problem.[1] The approach employed sets the entire heater in node 1, and the slab is divided into NEL-1 additional nodes shown below.

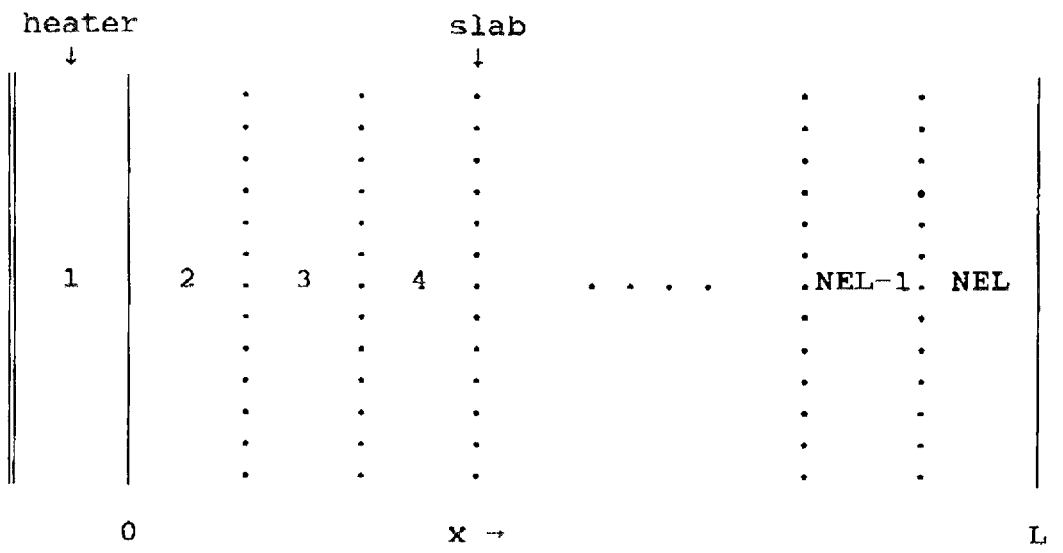

The model is developed from heat balances performed on each node.

NODE 1:

$$IN \quad = \quad OUT \quad + \quad ACCUMULATION$$

$$\frac{I^2 \cdot R}{2} = -kA \left.\frac{\partial t}{\partial x}\right|_{x=0} + V\rho C \frac{\partial T}{\partial t} \ . \tag{A1}$$

Written as a finite difference equation, this becomes

$$\frac{I^2 \cdot R}{2} = -kA \frac{T_2' - T_1'}{\Delta x/2} + V\rho C \frac{T_1' - T_1}{\Delta t} \ , \tag{A2}$$

where T_1' and T_1 are the temperature at position 1 and at times $t+\Delta t$ and t respectively. The thickness of all nodes except node 1 is

$$\Delta x = L/(NEL - 1) \ . \tag{A3}$$

The thickness of node 1 is 0.5 t_{sc}. The factor of ½ appears in the denominator of the first term on the right hand side of Eq. (A2) because the conductivity of the heater was assumed to be large compared with that of the slab (i.e., the heater is isothermal). Rearranging Eq. (A2) yields

$$(1 + TMR \cdot \Gamma)(T_1' - T_2') = \frac{I^2 \cdot R \cdot \Delta x}{4\,kA} + TMR \cdot \Gamma \cdot T_1 \ , \ where$$

$$TMR = t_{sc}\, \rho_{sc}\, C_{sc}/(4L\rho C) \ , \ and$$

$$\Gamma = \rho C \Delta x^2/(k\Delta t) \ .$$

NODE 2:

$$-kA \left.\frac{\partial T}{\partial x}\right|_{x=0} = -kA \left.\frac{\partial T}{\partial t}\right|_{x=\Delta x} + V\rho C \frac{\partial T}{\partial t} \ . \tag{A5}$$

Written in finite difference form, this equation becomes

$$-kA\frac{T_2'-T_1'}{\Delta x/2} = -kA\frac{T_3'-T_2'}{\Delta x} + V\rho C\frac{T_2'-T_2}{\Delta t} \tag{A6}$$

or

$$-2T_1' + (3 + \Gamma)T_2' - T_3^1 = \Gamma \cdot T' . \tag{A7}$$

NODES 3 to NEL-1:

$$-kA\frac{\partial T}{\partial x}\Big|_{x=x} = -kA\frac{\partial T}{\partial x}\Big|_{x=x+\Delta x} + V\rho C\frac{\partial T}{\partial t} . \tag{A8}$$

Written in finite difference form, this equation becomes

$$-kA\frac{T'_i-T'_{i-1}}{\Delta x} = -kA\frac{T'_{i+1}-T'_i}{\Delta x} + V\rho C\frac{T'_i-T_i}{\Delta t} \tag{A9}$$

or

$$-T'_{i-1} + (2 + \Gamma)T'_i - T'_{i+1} = \Gamma \cdot T_i . \tag{A10}$$

NODE NEL:

$$-kA\frac{\partial T}{\partial x}\Big|_{x=L-\Delta x} = -kA\frac{\partial T}{\partial x}\Big|_{x=L} + V\rho C\frac{\partial T}{\partial t} . \tag{A11}$$

Written in finite difference form, this equation becomes

$$-kA\frac{T'_{NEL} - T'_{NEL-1}}{\Delta x} = -kA\frac{T(0) - T'_{NEL}}{\Delta x/2} + V\rho C\frac{T'_{NEL} - T_{NEL}}{\Delta t} . \qquad \text{(A12)}$$

or

$$-T'_{NEL-1} + (3 + \Gamma)\,T'_{NEL} = \Gamma \cdot T_{NEL} + 2T(0) \qquad \text{(A13)}$$

Equation (A4) for node 1, Eq. (A7) for node 2, Eq. (A10) for nodes 3 through NEL-1, and Eq. (A13) for node NEL form a set of NEL linear equations with NEL unknowns (i.e., the temperature of the nodes at each time increment). The following FORTRAN program solves the equations at each time increment and stores the heater temperature.

Finite difference program to analyze the effect of the screen thermal mass on the temperature response of the screen

```
      REAL K, L
      CHARACTER*12 ZFILE
      DIMENSION A(101), B(101), C(101), D(101), T(101),
     1 TIME (1000), T0(1000)
      WRITE (*,199)
  199 FORMAT (2X, 'INPUT NAME OF OUTPUT FILE')
      READ (*,'(A12)') ZFILE
      OPEN(2, FILE=ZFILE, STATUS='NEW')
      WRITE (*,200)
  200 FORMAT (' INPUT NEL, IFREQ, DTAU, TC, TSAZERO, CP, RHO, K, L, TMR
     1, FS AND TAUMAX')
      READ (*,*) NEL, IFREQ, DTAU, TC, TSAZERO, CP, RHO, K, L, TMR,
     1 FS, TAUMAX
      NM1 = NEL - 1
      FN = NEL
      FNM1 = NM1
      DX = L / FNM1
      GAMMA = (CP*RHO/K)*DX*DX/DTAU
      B(1) = 1. +TMR*GAMMA
      C(1) = -1.0
      T(1) = TSAZERO
      DO 2 I =2,NEL
      FI = I
      A(I) = -1.0
      B(I) = 2.0 + GAMMA
      C(I) = -1.0
    2 T(I) = TSAZERO + ( TC - TSAZERO ) * (FI-1.5) / FNM1
      A(2) = -2.
      B(2) = 3. + GAMMA
      B(NEL) = 3 + GAMMA
      C(NEL) = 0
      ICOUNT = 0
      TAU = 0.0
      IPRINT = 1
      TIME (IPRINT) = TAU
      T0(IPRINT) = T(1)
      WRITE (*,201)
  201 FORMAT (' INITIALIZATION COMPLETE')
    3 TAU = TAU + DTAU
      WRITE (*,*) TAU, T(1)
      ICOUNT = ICOUNT + 1
      D(1) = FS*DX/(4*K)+TMR*GAMMA*T(1)
```

Finite difference program (cont'd)

```
      DO 6 I=2,NEL
    6 D(I) = GAMMA*T(I)
      D(NEL) = D(NEL) + 2 * TC
      CALL TRIDIAG (1, NEL, A, B, C, D, T)
      IF (ICOUNT .NE. IFREQ) GO TO 8
      IPRINT = IPRINT + 1
      TIME (IPRINT) = TAU
      T0(IPRINT) = T(1)
      ICOUNT = 0
    8 CONTINUE
      IF ( TAU .GE. TAUMAX ) GO TO 10
      GO TO 3
   10 WRITE (2,205) NEL, IFREQ, DTAU, TC, TSAZERO, CP, RHO, K, L, TMR,
     1 FS, TAUMAX, (TIME(I), T0(I),  I=1,IPRINT)
  205 FORMAT (' INPUT DATA ',/,' NEL, IFREQ, DTAU, TC, TSAZERO, CP,
     1 RHO, K, L, TMR, FS, AND TAUMAX ',/, I3, 2X, I3, 2X, 7F10.3, /,
     2 F12.5, 2F10.3, //, ' RESULTS',/, ' TIME(I), T0(I)', /,
     3 (2F12.3))
      STOP
      END
      SUBROUTINE TRIDIAG (IF, L, A, B, C, D, V)
      DIMENSION A(1), B(1), C(1), D(1), V(1), BETA(101), GGAMMA(101)
      BETA(IF) = B(IF)
      GGAMMA(IF) = D(IF)/BETA(IF)
      IFP1 = IF + 1
      DO 1 I=IFP1,L
      IM1 = I - 1
      BETA(I) = B(I)-A(I)*C(IM1)/BETA(IM1)
    1 GGAMMA(I) = (D(I)-A(I)*GGAMMA(IM1))/BETA(I)
      V(L) = GGAMMA(L)
      LAST = L - IF
      DO 2 K=1,LAST
      I = L - K
      IP1 = I + 1
    2 V(I) = GGAMMA(I) -C(I) * V(IP1)/BETA(I)
      RETURN
      END
```

The required inputs to this program are:

ZFILE	file name for the calculated results
NEL	1 plus the number of nodes in the slab
IFREQ	IFREQ • DTAU equals the time interval between outputting results, s
DTAU	time increment in solution, s
TC	temperature at x equal L, °C
TSAZERO	initial heater temperature, °C
CP	slab specific heat, J/kg•K
RHO	slab density, kg/m^3
K	slab thermal conductivity, W/m•K
L	slab thickness, m
TMR	see text for equation, dimensionless
FS	$\Delta I^2 \cdot R/A$, W/m^2
TAUMAX	maximum time interval, s

Sample inputs and the resulting outputs are shown below. The information that must be supplied by the user is indicated in brackets, < >.

Sample Inputs

```
INPUT NAME OF OUTPUT FILE
<TEST1.DAT>
INPUT NEL, IFREQ, DTAU, TC, TSAZERO, CP, RHO, K, L, TMR, FS, AND TAUMAX
<51>
<12>
<1>
<25>
<30>
<1000.>
<30.>
<0.02>
<0.05>
<0.025>
<5.>
<120>
```

Sample Output

```
NEL, IFREQ, DTAU, TC, TSAZERO, CP, RHO, K, L, TMR, FS, AND TAUMAX
51   12   1.000   25.000   30.000   1000.000   30.000   0.020   0.050
0.25000   10.000   120.000
```

RESULTS
TIME (I), T0(I)

0.000	30.000
12.000	30.410
24.000	30.607
36.000	30.758
48.000	30.886
60.000	30.998
72.000	31.100
84.000	31.914
96.000	31.194
108.000	31.364
120.000	31.441

Stop - Program terminated.

Reference

1. B. Carnahan, H. A. Luther, and J. O. Wilkes, Applied Numerical Techniques, Wiley, New York, 1972, 465–73.

APPENDIX B

PROGRAM THAT PERFORMS THE ITERATIVE CALCULATIONS FOR METHOD 3

Because C appears on both sides of Eq. (12) (i.e., on the left as C and in the denominator of TMR), an iterative technique was employed to solve the equation. The solution starts with a guess for C equal to $\{F/[(\pi \bullet \rho \bullet k)^{0.5}\ S(TMR)]\}^2$. This value for C is then used to calculate a value for TMR. The value for TMR is then used to find a new value for C using Eq. (12). The iteration continues until the new C and old C values agree to 0.001%. The FORTRAN program that performs the iterative solution of Eq. (12) is given below.

```
      REAL K, L
      WRITE (*,100)
  100 FORMAT (2X, 'INPUT SLOPE@TMRP, K, L, RHO AND POWER')
      EPS = 0.00001
      IMIN = 10
      IMAX = 1000
      TSCR = 0.00066
      RHOSCR = 2035.
      CSCR = 435.
      READ (*,*) SLOPE, K, L, RHO, FS
      CSTART = (FS/SLOPE)**2/(3.14159265*RHO*K)
      COLD = CSTART
      I = 0
    1 TMRP = ((TSCR/2.)*RHOSCR*CSCR)/(L*RHO*COLD)
      I = I + 1
      CORR = 0.999627-0.0969039*TMRP-2.61173*TMRP**2+5.46615*TMRP**3
      IF (TMRP .GT. 0.2) CORR = 1.02572-0.574271*TMRP+0.191186*TMRP**2
      C = CSTART*CORR**2
      CEPS = ABS(C/COLD-1.)
      IF (CEPS .LT. EPS .AND. I .GE. IMIN) GO TO 2
      IF ( I .GT. IMAX ) GO TO 3
      COLD = C
      GO TO 1
    2 WRITE (*,101) C, TMRP
  101 FORMAT (2X, 'C EQUALS ', F8.2, '  TMRP EQUALS  ', F7.3)
    3 STOP
      END
```

The required inputs are as follows:

SLOPE	slope @ $0.3 \leq \bar{T} \leq 0.5$, S (TMR)
K	slab thermal conductivity, W/m•K
L	slab thickness, m
RHO	slab density, kg/m^3
FS	$\Delta I^2 \bullet R/A$, W/m^2

Sample inputs and the resulting output are shown below. The user supplied inputs are shown in brackets, < >.

Sample Inputs

INPUT SLOPE @ TMR, K, L, RHO, AND POWER

<0.2>
<0.02>
<0.05>
<30.>
<10.>

Sample Output

C EQUALS 1161.21 TMRP EQUALS 0.168
Stop - Program terminated.

INTERNAL DISTRIBUTION

1-2. Central Research Library
3. Document Reference Section
4-5. Laboratory Records Department
6. Laboratory Records, ORNL RC
7. ORNL Patent Section
8-10. M&C Records Office
11. C. Brown
12-16. G. L. Burn
17. R. S. Carlsmith
18. K. W. Childs
19. J. Christian
20. J. L. Cook
21. J. W. Cooke
22. G. E. Courville
23. D. F. Craig
24. R. B. Dinwiddie
25-29. H. A. Fine
30-34. R. S. Graves
35. J. A. Horton, Jr.
36. T. G. Kollie
37. M. A. Kuliasha
38. W. D. Porter
39-43. D. L. McElroy
44. H. A. McLane
45. C. E. Weaver
46. K. E. Wilkes
47-51. D. W. Yarbrough
52. A. D. Brailsford (Consultant)
53. Y. A. Chang (Consultant)
54. H. W. Foglesong (Consultant)
55. J. J. Hren (Consultant)
56. M. L. Savitz (Consultant)
57. J. B. Wachtman, Jr. (Consultant)

EXTERNAL DISTRIBUTION

58. ARASTEH, DARIUSH, 90-3111, LBL, Berkeley, CA 94720

59. ARIZONA STATE UNIVERSITY, Mechanical and Aerospace Engineering, Tempe, AZ 85287

    T. W. Long (Professor)

60. BANKVALL, CLAES, SP, P.O. Box 857, S-50115, Boras, Sweden

61. BARRIER SYSTEM, W. Seneca Ave., P.O. Box 346, Canastota, NY 13032-0346

    B. Brod

62. BASF CANADA INC., 345 Carlingview Drive, Toronto, Ont. M9W 6N9 CANADA

    T. Harris

63. BAUMGARDNER, R. L., P.O. Box 308, Stroudsburg, PA 18360

64. CELOTEX CORPORATION, 4010 Boy Scout Blvd., Tampa, FL 33607

S. A. Funk, AIA, PE, RCI

65. CERTAINTEED CORPORATION, P.O. Box 860, Valley Forge, PA 19482

M. B. Lacher

66. CERTAINTEED CORPORATION, 1400 Union Meeting Road, Blue Bell, PA 19422

D. J. McCaa

67. CTL, 5420 Old Orchard Road, Skokie, IL 60077

M. G. Van Geem

68-70. DOW CHEMICAL USA, P.O. Box 515, Granville, OH 43023

J. H. Minsker
D. L. Roodvoets
M. Weick

71. EDMUNDS, W. M., 2790 Columbus Road, Granville, OH 43023

72. ELLIS, W. P., Standards Consultant, 754 Bob-Bea Lane, Harleysville, PA 19438

73. E.P.A. (ANR-445), Global Change Division, 401 M. Street, S.W., Washington, DC 20460

A. Fine

74. FEDERAL TRADE COMMISSION, (Room S-4631), Sixth & Pennsylvania Avenue NW, Washington, DC 20580

K. Howerton

75. FOAM ENTERPRISES, 13630 Watertower Circle, Minneapolis, MN, 55441

J. Andersen

76. FRENCH ENGINEERING, INC., 4511 Dawn Creek, Spring, TX 77388

W. R. French, P.E.

77. GEOSCIENCE LTD., 410 South Cedros Avenue, Solana Beach, CA 92075

H. F. Poppendiek

78. GILBO, C. F., 1820 Westcott Drive, Lancaster, PA 17603

79. HOLOMETRIX, INC., 99 Erie Street, Cambridge, MA 02139

A. Desjarlais

80. JPS ELASTOMERICS, 395 Pleasant Street, Northampton, MA 01060

E. Riley

81-82. JIM WALTER RESEARCH CORPORATION, 10301 Nineth Street North, St. Petersburg, FL 33716

J. R. Hagan
R. G. Miller

83. LaCOSSE, R.A., 207 Withorn Lane, Mt. Prospect, IL 60056

84. LEGER DESIGNS, 256 Middle Branch Road, New Boston, NH 03070

G. Leger

85. MANVILLE SALES CORPORATION, R-46, P.O. Box 5108, Denver, CO 80217

D. G. Ober

86. MASSACHUSETTS INSTITUTE OF TECHNOLOGY, Rm. 3-433, 77 Mass Avenue, Cambridge, MA 02139

L. R. Glicksman

87. MICHIGAN STATE UNIVERSITY, Department of Mechanical Engineering, A231, East Lansing, MI 48824

J. V. Beck (Professor)

88. MIMA, 1420 King Street, Alexandria, VA 22314

S. Braun

89-90. MOBAY CORPORATION, Mobay Road, Pittsburgh, PA 15205

M. Bassi
D. C. Wysocki

91. NAHB NATIONAL RESEARCH CENTER, 400 Prince Georges Blvd., Upper Marlboro, MD 20772

R. S. Sikand

92. NATIONAL ASSOCIATION OF HOME BUILDERS, 15th & M Streets, NW, Washington, DC 20005

J. A. Smith (Energy Program Manager)

93. NATIONAL INSTITUTE OF STANDARDS AND TECHNOLOGY, Acoustic Measurements Group, Building 233, Room A149, Gaithersburg, MD 20899

D. R. Flynn (Leader)

94-95. NATIONAL RESEARCH COUNCIL CANADA, Building Performance Section, Institute for Research in Construction, Ottawa, Ontario K1A 0R6 CANADA

M. Bomberg (Senior Researcher)
W. C. Brown

96. NAVAL CIVIL ENGINEERING LABORATORY, Port Hueneme, CA 93043

R. L. Alumbaugh

97. NEW JERSEY INSTITUTE OF TECHNOLOGY, Bear Center, Newark, NJ 07102

E. Bales

98. NEW YORK STATE ENERGY OFFICE, 2 Rockefeller Plaza, Albany, NY 12223

D. R. Abrey

99. NIST, 325 Broadway, Boulder, CO 80303-3328

D. R. Smith

100. NIST, Building 226, B-320, Gaithersburg, MD 20878

R. Zarr

101. NRG BARRIERS, INC., 15 Lund Road, Saco, ME 04072-1859

J. L. Clinton

102-103. OWENS-CORNING FIBERGLAS, 2790 Columbus Road, Rt. 16, Granville, OH 43023-1200

M. McBride
J. R. Mumaw

104. PLYMOUTH FOAM PRODUCTS, P.O. Box 407, 1800 Sunset Drive, Plymouth, WI 53073

V. Roberts

105. PORTLAND STATE UNIVERSITY, Mechanical Engineering Department, Portland, OR 97207

G. Tsongas

106. POWELL, F. J., 12218 Cattail Lane, Jacksonville, FL 32223

107. PROGRESSIVE ARCHITECTURE, 600 Summer Street, Stanford, CT 06904

K. Labs

108. REGAL INDUSTRIES, Rt. 1, Box 46, Crothersville, IN 47229

D. McGuire

109. REMAX, INC., 13524 Welch Road, Dallas, TX 75244-5291

H. J. Roberts, Jr.

110. ROOF DESIGN WORKS, INC., 516 Renford Drive, Knoxville, TN 37919

W. F. Martin

111. ROOF MAINTENANCE SYSTEMS, P.O. Box 67, Farmingdale, NJ 07727

R. Martin (President)

112. ROOFING SERVICES, INC., 6106 Roxbury Avenue, Springfield, VA 22152-1621

F. C. Gorham

113. SHERMAN, M., 6723 14th Avenue North, St. Petersburg, FL 33710-5405

114. SMALL HOMES COUNCIL, 1 E St. Mary's Road, Champaign, IL 61820

S. Tewes

115. SOCIETY OF THE PLASTICS INDUSTRY, INC., Polyurethane Division, 355 Lexington Avenue, New York, NY 10017

F. W. Lichtenberg

116. STERN, E., 5386 West Broadway, Montreal, Quebec, Canada H4V 2A4

117. STEVEN WINTER ASSOCIATES INC., Building Systems Consultant, 50 Washington Street, Norwalk, CT 06854

A. Tuluca

118. SWEDISH INSTITUTE FOR BUILDING RESEARCH, P.O. Box 785, Gavle, Sweden S-80129

M. D. Lyberg

119. THERMAL PRODUCTS INTER., 1020 Wm. Pitt Way, Pittsburgh, PA 15238

D. E. Emmert (General Manager)

120. TREMCO, INC., 10701 Shaker Blvd., Cleveland, OH 44104

D. C. Portfolio

121. TYE, R. P., 292 Jerusalem Road, Cohasset, MA 02025

122. UC INDUSTRIES, 137 East Avenue, Box 423, Tallmadge, OH 44278

B. Wojtechko

123. UNDERGROUND SPACE CENTER, 500 Pillsbury Drive SE, Minneapolis, MN 55455

R. L. Sterling

124. UNIVERSITY OF MASSACHUSETTS, Mechanical Engineering Department, Amherst, MA 01003

W. P. Goss

125. UNIVERSITY OF MISSISSIPPI, Mechanical Engineering, University, MS 3677

J. A. Roux

126. UNIVERSITY OF PITTSBURGH, Mechanical Engineering Department, 648 Benedum Hall, Pittsburgh, PA 15261

R. S. Dougall

127. VANDER LINDEN & ASSO., 5 Brassie Way, Littleton, CO 80123

C. R. Vander Linden

128. U. S. DEPARTMENT OF ENERGY , Oak Ridge Operations Office, P.O. Box 2008, Oak Ridge, TN 37831-8600

Assistant Manager for Energy Research and Development

129-138. U. S. DEPARTMENT OF ENERGY, Office of Scientific and Technical Information, P. O. Box 62, Oak Ridge, TN 37831

For distribution by microfiche as shown in DOE/OSTI-4500, Distribution Category UC-350 (Energy Conservation in Buildings).